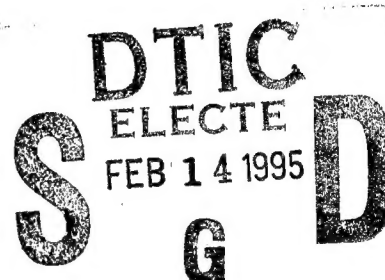# CHEMICALLY INDUCED PASSIVITY OF ALUMINUM ALLOYS AND AL-BASED METAL MATRIX COMPOSITES

F. Mansfeld and Y. Wang
Corrosion and Environmental Effects Laboratory
Department of Materials Science and Engineering
University of Southern California
Los Angeles, CA 90089-0241

DTIC
ELECTE
FEB 1 4 1995
S
G
D

JANUARY 1995

Final Report for the period:
October 1, 1990 to September 30, 1994
Contract No. N00014-91-J-1041

DTIC QUALITY INSPECTED 3

19950206 216

REPORT DOCUMENTATION PAGE

Public reporting burden for this collection of information is estimated to average 1 hour per response, including the time for reviewing instructions, searching existing data sources, gathering and maintaining the data needed, and completing and reviewing the collection of information. Send comments regarding this burden estimate or any other aspect of this collection of information, including suggestions for reducing this burden, to Washington Headquarters Services, Directorate for Information Operations and Reports, 1215 Jefferson Davis Highway, Suite 1204, Arlington, VA 22202-4302, and to the Office of Management and Budget, Paperwork Reduction Project (0704-0188), Washington, DC 20503.

1. AGENCY USE ONLY (Leave blank)	2. REPORT DATE	3. REPORT TYPE AND DATES COVERED

4. TITLE AND SUBTITLE

Chemically Induced Passivity of Aluminum Alloys and Al-Based Metal Matrix Composites

5. FUNDING NUMBERS

N00014-91-J-1041

6. AUTHOR(S)

Florian Mansfeld

7. PERFORMING ORGANIZATION NAME(S) AND ADDRESS(ES)

University of Southern California
Materials Science Department
University Park
Los Angeles, CA 90089-0241

8. PERFORMING ORGANIZATION REPORT NUMBER

1

9. SPONSORING / MONITORING AGENCY NAME(S) AND ADDRESS(ES)

Office of Naval Research
800 N. Quincy Street
Arlington, VA 22217-5660
Attn: Code 3310

10. SPONSORING / MONITORING AGENCY REPORT NUMBER

11. SUPPLEMENTARY NOTES

12a. DISTRIBUTION / AVAILABILITY STATEMENT

Approved for Public Release: Distribution Unlimited

12b. DISTRIBUTION CODE

13. ABSTRACT (Maximum 200 words)

The concept of surface modification has been applied for corrosion protection of commercial aluminum alloys such as Al 2024, Al 6013, Al 6061 and Al 7075. The goal of this project was to develop methods of corrosion protection which do not use toxic chemicals. The Ce-Mo process consisting of immersion in hot solutions of $CeCl_3$ and $Ce(NO_3)_3$ followed by anodic polarization in a molybdate solution has produced surfaces with exceptional resistance to localized corrosion for Al 6013 and 6061. Surface modified samples did not pit during exposure to 0.5 M NaCl for 30 days. For Al 2024 and Al 7075 it was found that a copper removal pretreatment step was necessary for complete corrosion protection. For Al 2024 replacement of $CeCl_3$ by Ce acetate produced optimum results. Surface analysis showed that both Ce and Mo are incorporated in the modified surface layers. For Al 7075 it was found that increased concentrations of Ce and Mo occur at sites where Cu containing particles are located. It is assumed that the exceptional corrosion resistance is in part due to elimination of local cathodes during the Ce-Mo process. Anodic polarization curves for Al 2024 and Al 7075 showed that the pitting potential E_{pit} was increased after surface modification, while the corrosion potential E_{corr} remained constant. Apparently the

14. SUBJECT TERMS

surface modification, corrosion protection, aluminum alloys, pitting, EIS, surface analysis.

15. NUMBER OF PAGES

16. PRICE CODE

17. SECURITY CLASSIFICATION OF REPORT	18. SECURITY CLASSIFICATION OF THIS PAGE	19. SECURITY CLASSIFICATION OF ABSTRACT	20. LIMITATION OF ABSTRACT
UNCLASSIFIED	UNCLASSIFIED	UNCLASSIFIED	UNCLASSIFIED

con't of abstract

amount of adsorbed Cl⁻ at a given potential is reduced in the presence of negatively
charged Mo species in the modified surface layers.

Accesion For		
NTIS CRA&I	☒	
DTIC TAB	☐	
Unannounced	☐	
Justification		
By		
Distribution /		
Availability Codes		
Dist	Avail and / or Special	
A-1		

TABLE OF CONTENTS

ABSTRACT

The concept of surface modification has been applied for corrosion protection of commercial aluminum alloys such as Al 2024, Al 6013, Al 6061 and Al 7075. The goal of this project was to develop methods of corrosion protection which do not use toxic chemicals. The Ce-Mo process consisting of immersion in hot solutions of $CeCl_3$ and $Ce(NO_3)_3$ followed by anodic polarization in a molybdate solution has produced surfaces with exceptional resistance to localized corrosion for Al 6013 and 6061. Surface modified samples did not pit during exposure to 0.5 M NaCl for 30 days. For Al 2024 and Al 7075 it was found that a copper removal pretreatment step was necessary for complete corrosion protection. For Al 2024 replacement of $CeCl_3$ by Ce acetate produced optimum results. Surface analysis showed that both Ce and Mo are incorporated in the modified surface layers. For Al 7075 it was found that increased concentrations of Ce and Mo occur at sites where Cu containing particles are located. It is assumed that the exceptional corrosion resistance is in part due to elimination of local cathodes during the Ce-Mo process. Anodic polarization curves for Al 2024 and Al 7075 showed that the pitting potential E_{pit} was increased after surface modification, while the corrosion potential E_{corr} remained constant. Apparently the amount of adsorbed Cl$^-$ at a given potential is reduced in the presence of negatively charged Mo species in the modified surface layers.

I. INTRODUCTION

Localized corrosion in the form of pitting is one of the most common failures of Al alloys. In engineering applications, protective surface treatments such as chromate conversion coatings, polymer coatings or anodizing have to be applied to obtain the desired service life.

In its pure state, when exposed to oxidizing environments, such as oxygen, water and the atmosphere, aluminum is protected by an air-formed oxide film which provides fair corrosion resistance. In most requirements, aluminum needs to be alloyed with constituents such as copper, magnesium, silicon, manganese, nickel, and zinc to enhance its mechanical strength. Among these constituents, copper is the principal alloying element giving the highest possible strength-to-weight ratios [1,2]. However, in terms of corrosion resistance, alloying markedly increases the susceptibility to localized corrosion. The corrosion resistance of Al alloys depends largely on their composition, highly alloyed/higher strength Al alloys being less corrosion resistant than commercially pure aluminum (99.5-99.79%), and therefore having increased need for protective surface treatments [3,4].

Al alloys can be protected against corrosion by a various methods of surface modification such as anodizing, chromate conversion coatings and organic finishing [5-8]. Chromate conversion coatings are used primarily by the aluminum finishing industry for domestic appliances, aircraft parts, and electronic equipment to enhance the adhesion of paint or other organic finishes or to improve corrosion resistance for Al alloys serving in corrosive atmospheres such as marine environments [9-12].

Chromate conversion coatings are being used extensively to protect Al alloys as construction and airframe materials. Chromium is among the EPA's top toxic substances. In its hexavalent form (Cr^{6+}) it is a known carcinogen, and its compounds are environmentally hazardous as waste products [13-15]. Current environmental legislation is moving towards to total exclusion of Cr^{6+} and tightening regulatory pressure to reduce the hazardous wastes of chromium compounds. Therefore, many attempts are made at present to increase the corrosion resistance of

Al alloys using non-toxic alternatives of Cr^{6+} [16-20].

In the search for chromate alternatives, attention first centered on metal oxyanion analogs of chromate, such as molybdates, tungstates, vanadates and permanganates. The most widely investigated of this group have been molybdates, mainly because of their non-toxic nature [16,17,21-24]. Mo as alloying element and as inhibitor provides corrosion protection for metals such as carbon steels [16,17]. As inhibitors, molybdate is widely used to protect ferrous and nonferrous metals in diverse corrosive environments. Mo is effective in inhibiting pitting and crevice corrosion, both as and alloying element and when added as MoO^{2-}_4 [16-18, 25-27]. The most important oxidation state of molybdenum is MoO^{2-}_4, which can form a variety of compounds with oxides of other metals [28]. As an alternative for Cr^{6+}, molybdate coatings for Al alloys have become interesting recently in corrosion engineering [18,29].

Molybdate coatings produced either by anodic polarization or by simple immersion in molybdate-containing solutions provide some corrosion protection for Al alloys [29-32]. Alloying Al with Mo by ion implantation improves the resistance of Al to localized corrosion by shifting the pitting potential E_{pit} in the noble direction [25,29], but from an engineering point of view, ion implantation has practical limitations due to its difficulty of application to large samples.

In the proceedings of a recent workshop on chromate replacements in light metal finishing results from efforts to develop Cr^{6+}-free conversion coatings for Al alloys using simple low-cost, non-toxic chemicals were summarized. It is apparent that so far no simple process is available which can completely replace chromate conversion coatings at equal corrosion resistance of the coated alloy and equal ease of application [33].

Efforts made in this investigation [34] have been devoted to provide corrosion protection for Al alloys without the use of toxic materials. The Ce-Mo processes based on the concept of surface modification were developed leading to "stainless Al alloys" with exceptional resistance to localized corrosion. The details of the particular surface modification procedure depend on alloy composition. For corrosion protection of Al alloys such as Al 6061, Al 6013 and pure Al surface modification consisted of immersion in boiling $Ce(NO_3)_3$, immersion in boiling $CeCl_3$ and anodic polarization in Na_2MoO_4. For high-Cu Al alloys such as Al 7075 and Al 2024, surface modification involved immersion in boiling $Ce(NO_3)_3$, anodic polarization in Na_2MoO_4 and immersion in boiling $CeCl_3$. A further modification of the Ce-Mo process which was very effective for Al 2024 consisted of immersion in hot $(CH_3CO_2)_3Ce$, anodic polarization in Na_2MoO_4 and immersion in hot $Ce(NO_3)_3$. Evaluation of corrosion resistance with EIS demonstrated that for surface modified Al alloys exposed to 0.5 M NaCl impedance spectra were capacitive and localized corrosion was not detected for the entire test period of at least 30 days. Polarization curves indicated that the increased resistance to pitting was due to increased E_{pit} at constant open-circuit potential E_{corr}. Surface analysis indicated that Ce and Mo were present in the modified surface layers and were concentrated at sites where alloying constituent particles such as Cu were located.

2. EXPERIMENTAL APPROACH

Several surface modification procedures using cerium salts combined with molybdate were developed and applied to Al and commercial Al alloys. The corrosion behavior of untreated and modified surfaces exposed to 0.5 M NaCl was monitored with EIS. Potential and current noise data were collected to obtain additional information concerning uniform and localized corrosion

process. The corrosion kinetics and the susceptibility to pitting were evaluated by polarization techniques. Surface analysis was performed by SEM, AES and EDS. Elemental mapping was used to identify the distribution of chemical components, especially Ce and Mo, in modified surface oxide layers.

2.1 Materials

The commercial Al alloys Al 6061-T6, Al 6013, Al 7075-T6, Al 2024-T3, and pure Al were studied. For the three commercial alloys Al 2024-T3, Al 6061-T6 and Al 7075-T6, the minor alloying elements are given in Table I.

2.2 Surface Preparation

Samples were usually cut into a size 7 x 7 cm^2 from 0.16 cm thick Al alloy sheets. The surfaces were carefully selected before each experiment to avoid surface defects due to mechanical damage or corrosion during prior exposure to the atmosphere. Surface conditions including as-received, deoxidized and polished were used in this investigations. As-received samples were degreased only with degreasing detergent, polished surfaces were prepared by silicon carbide paper finishing with 1200 grit, and deoxidized surfaces were prepared by immersion in Diversey 560 solution (Diversified Chemical Sales, Inc., USA) at room temperature for 10 minutes followed by rinsing with distilled water. The major chemicals contained in Diversey 560 are listed in Table II.

2.3 Solution Preparation

For high-Cu Al alloys, Cu removal pretreatment was applied before surface modification by one of the Ce-Mo processes. The solution for Cu removal from Al 2024 by the chemical method was prepared with 22.8 g/l Deoxidizer 7, 100 ml/l H_3PO_4 and distilled water. For Cu removal from Al 2024 by the electrochemical method, 0.5 M $NaNO_3$ with addition of 100 ml/l HNO_3 was used, while for Al 7075 a 0.5 M $NaNO_3$ solution was used and the pH was adjusted to 1 with HCl.

The corrosion test solution of 0.5 M NaCl and the treatment solutions 4 mM $(CH_3CO_2)_3Ce$, 5 mM $CeCl_3$, 10 mM $Ce(NO_3)_3$ and 0.1 M Na_2MoO_4, were prepared with distilled water from chemicals of AR grade. The pH values of these solutions (as prepared) are listed in Table III.

2.4 Cu Removal Processes

Two Cu removal processes, categorized as the chemical process and the electrochemical process, have been developed previously at CEEL. The electrochemical Cu removal process consists of deoxidizing in Diversey 560 for 10 minutes at room temperature, followed by anodic polarization in a Cu removal solution (Table IV). In the polarizing step, different operation parameters were used for Al 2024 and Al 7075. Al 2024 was polarized at -55 mV (vs. SCE) in 0.5 M $NaNO_3$ + 0.67 M HNO_3, while for Al 7075 a potential of -248 mV was applied in 0.5 M $NaNO_3$ (pH = 1 adjusted by HCl).

Table I. Minor alloying elements for Al alloys (wt %)

Element	Al 2024-T3	Al 6061-T6	Al 7075-T6
Cu	3.8 - 4.9	0.15 - 0.40	1.2 - 2.0
Si	<0.50	0.4 - 0.8	<0.40
Fe	<0.50	<0.70	<0.50
Mn	0.3 - 0.9	<0.15	<0.30
Mg	1.2 - 1.8	0.8 - 1.2	2.1 - 2.9
Zn	<0.25	<0.25	5.1 - 6.1
Cr	<0.10	0.04 - 0.35	0.18 - 0.28
Ti	<0.15	<0.15	<0.20

Table II. Chemical composition of Diversey 560

Chemical	Content (w/o %)
HNO_3	<15
H_2SO_4	<25
H_2SiF_7	< 2

Table III. pH values of test and treatment solutions

Solution	pH
0.5 M NaCl	6.5 - 6.8
4 mM $(CH_3CO_2)_3Ce$	6.8 - 6.9
5 mM $CeCl_3$	5.7 - 5.9
10 mM $Ce(NO_3)_3$	4.5 - 4.8
0.1 M Na_2MoO_4	9.8 - 10.7

Table IV. Electrochemical process for Cu removal

Step	Al 2024-T3	Al 7075-T6
1. Cleaning and degreasing	Immersion in Alcoonox for 1 min.	Immersion in Alconox for 1 min
2. Deoxidizing	Diversey 560 for 10 min Rinse	Diversey 560 for 10 min Rinse
3. Copper removal	Polarization in 0.5 M $NaNO_3$ + 0.67 M HNO_3 at -55 mV (vs. SCE) for 30 min. Rinse	Polarization in 0.5 M $NaNO_3$, pH = 1 adjusted with HCl at -248 mV (vs. SCE) for 30 min. Rinse

2.5   Surface Modification Procedures

Surface modification of Al alloys using combined chemical and electrochemical processes includes three Ce-Mo processes. The original Ce-Mo process ("the Ce-Mo process") consists of baking at 100°C for 2 days after deoxidizing the surface, immersion in 10 mM $Ce(NO_3)_3$ and 5 mM $CeCl_3$, respectively, at 100°C for 2 hours, followed by polarization in 0.1 M Na_2MoO_4 at +500 mV vs SCE for 2 hours. The process parameters are listed in Table V. This original Ce-Mo process was used to modify the surface oxide layers on pure Al and Al 6061.

For Al 7075 and Al 2024 the surface modification process ("the modified Ce-Mo process #1") consists of immersion in boiling 10 mM $Ce(NO_3)_3$ at 100°C for 2 hours, anodic polarization in 0.1 M Na_2MoO_4 at +100 mV vs mercury sulfate reference electrode for 2 hours and immersion in 5 mM $CeCl_3$ at 100°C for 2 hours. Between each step, the surface was rinsed with distilled water (Table VI).

For surface modification of Al 2024, the modified Ce-Mo process #1 was further altered by reversing step 1 and step 3 in Table VI, and replacing $CeCl_3$ with $(CH_3CO_2)_3Ce$. The process steps for the modified Ce-Mo process #2 are described in Table VII. Anodic polarization curves for Al 2024, Al 6061 and Al 7075 in 0.1 M Na_2MoO_4 (open to air) are presented in Fig. 1. The applied potential of +500 mV vs. SCE during Mo treatment was selected to be in the passive region (Fig. 1).

2.6   Corrosion Tests

Corrosion behavior of Al alloys without and with surface modification was evaluated in 0.5 M NaCl (open to air) at room temperature. Electrochemical techniques such as EIS, polarization curves and electrochemical noise analysis were used to determine the kinetics and mechanisms resulting in improved pitting resistance. Surface analysis was performed to obtain detailed information concerning the surface chemistry and chemical concentration profiles of modified surface layers.

2.6.1 Corrosion Monitoring with EIS

EIS was used to monitor the corrosion process during exposure to 0.5 M NaCl. The EIS data were collected with a Schlumberger Model 1250 Frequency Response Analyzer (FRA) and a Schlumberger Model 1286 potentiostat controlled by a personal computer using the Z-plot software package (Scribner and Associates, Charlottesville, VA). Applied frequencies covered a range of 65 kHz to 1 mHz, a potential perturbation signal of 10 mV amplitude (peak to peak) was used. The measurements of EIS data were carried out at E_{corr}. Before starting a measurement, a delay time, usually 20 minutes, was applied to allow the system to stabilize.

The experimental EIS data were analyzed using BASICS and PITFIT software which was developed in this laboratory [35,36]. EIS spectra were usually either of capacitive or pitting type. Capacitive EIS spectra were analyzed using the BASICS software based on the one-time constant model of the EC shown in Fig. 2. For pitting corrosion, a transmission line impedance was usually obtained at low frequencies and the EIS data were in good agreement with the pitting model described in Fig. 3. In this case, the EIS data were analyzed using the PITFIT software [35,36].

Table V.   The Ce-Mo process

Step	Treatment
1. Oxidizing	Baking at 100°C for 2 days
2. Surface modification by Ce(NO$_3$)$_3$	Immersion in 10 mM Ce(NO$_3$)$_3$ at 100°C for 2 hours, then rinsing in distilled water
3. Surface modification by CeCl$_3$	Immersion in 5 mM CeCl$_3$ at 100°C for 2 hours, then rinsing in distilled water
4. Surface modification by Na$_2$MoO$_4$	Polarizing in 0.1 M Na$_2$MoO$_4$ at +500 mV (vs. SCE) for 2 hours, then rinsing in distilled water

Table VI.   The modified Ce-Mo process #1

Step	Treatment
1. Surface modification by Ce(NO$_3$)$_3$	Immersion in 10 mM Ce(NO$_3$)$_3$ at 100°C for 2 hours, then rinsing in distilled water
2. Surface modification by Na$_2$MoO$_4$	Polarizing in 0.1 M Na$_2$MoO$_4$ at +100 mV (vs. mercury sulfate reference electrode) for 2 hours, then rinsing in distilled water
3. Surface modification by CeCl$_3$	Immersion in 5 mM CeCl$_3$ at 100°C for 2 hours, then rinsing in distilled water

Table VII.   The modified Ce-Mo process #2

| Step	Treatment
1. Surface modification by (CH$_3$CO$_2$)$_3$Ce	Immersion in 4 mM (CH$_3$CO$_2$)$_3$Ce at 100°C for 2 hours, then rinsing in distilled water
2. Surface modification by Na$_2$MoO$_4$	Polarizing in 0.1 M Na$_2$MoO$_4$ at +100 mV (vs. mercury sulfate reference electrode) for 2 hours, then rinsing in distilled water
3. Surface modification by Ce(NO$_3$)$_3$	Immersion in 10 mM Ce(NO$_3$)$_3$ at 100°C for 2 hours, then rinsing in distilled water
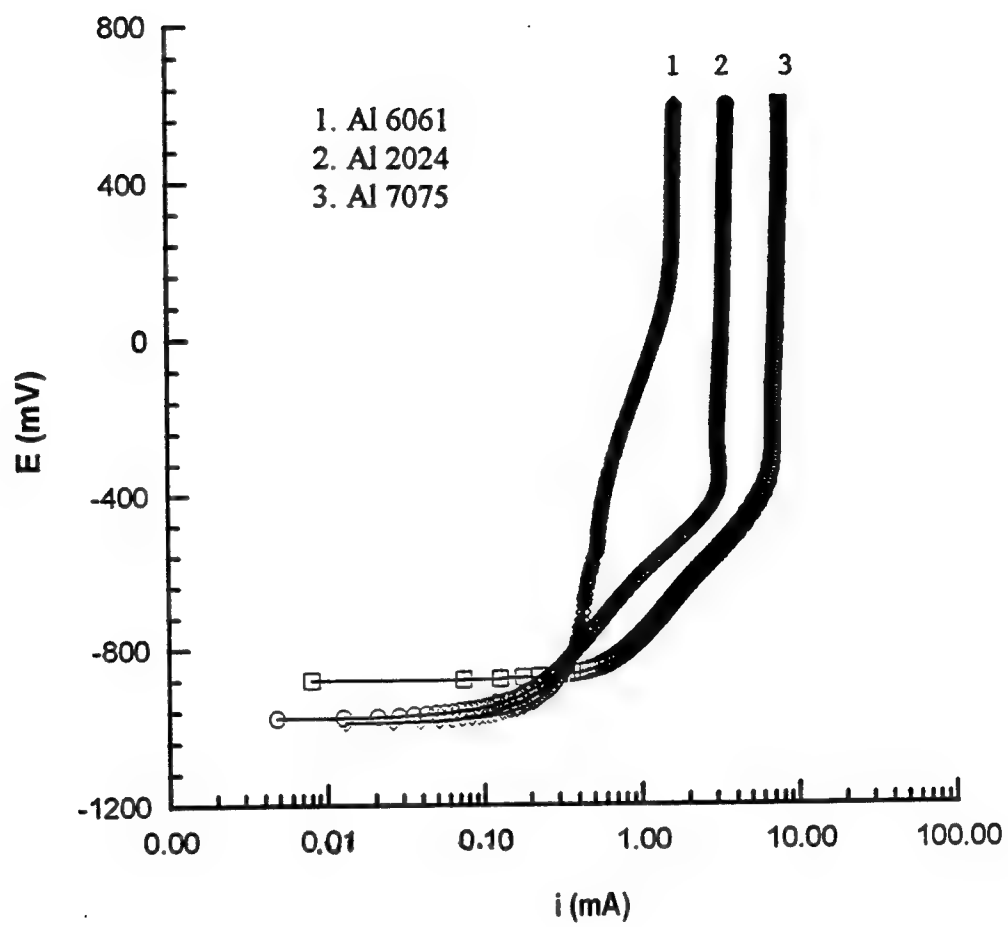
Fig. 1. Polarization curves for Al 6061 in aerated 0.1 M Na$_2$MoO$_4$
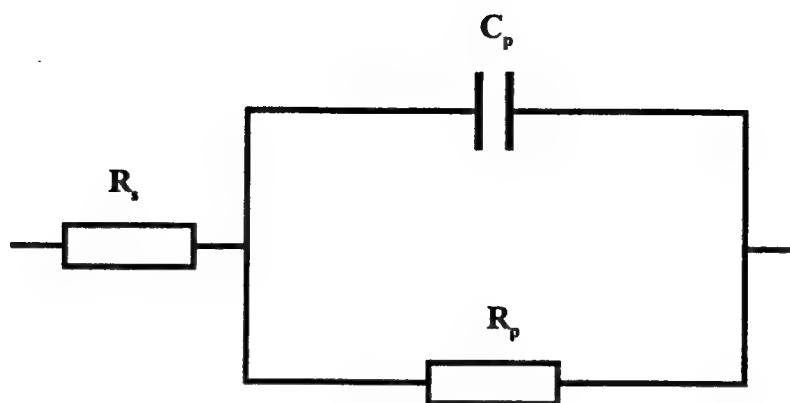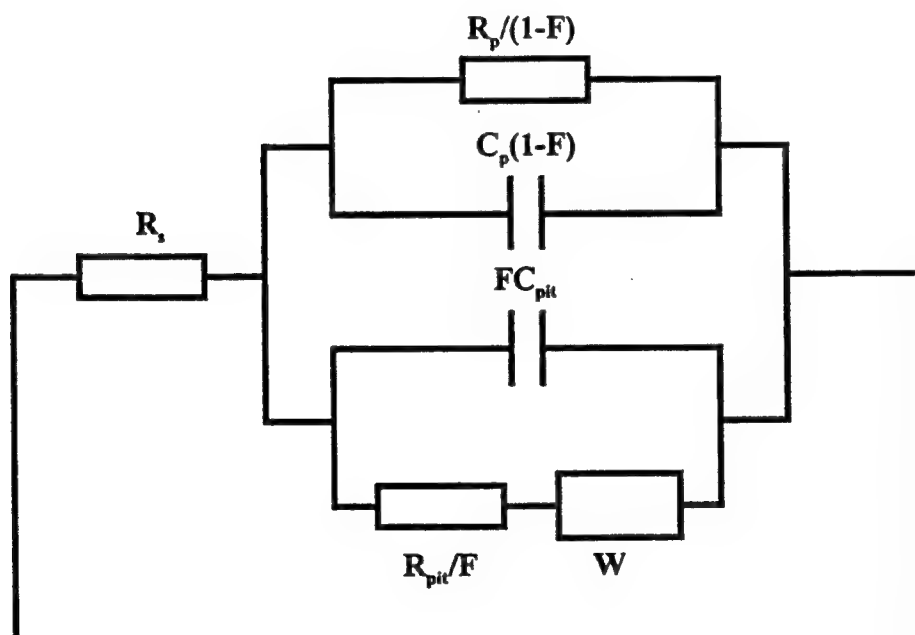
Fig. 2. Equivalent circuit for a passive surface

Fig. 3. Pitting model for Al alloys exposed to 0.5 M NaCl

2.6.2 Polarization Curves

Polarization curves for both as-received and modified Al alloys were measured in 0.5 M NaCl (open to air) by the potentiodynamic polarization technique. The measuring system consisted of a Princeton Applied Research (PAR) potentiostat Model 173 with a Model 376 interface operated by an IBM compatible computer using PAR 342C software.

Recording of polarization curves was started after immersion in the test solution for at least 40 minutes when E_{corr} had become stable. The anodic polarization curve was measured from E_{corr} -20 mV to E_{corr} +300 mV. The cathodic polarization curve was measured from E_{corr} + 10 mV to E_{corr} - 400 mV. The scan rate was at 0.2 mV/s. The exposed area of the working electrode was 5 cm^2. From the anodic or cathodic polarization curves, E_{pit}, passive current density i_p and cathodic limit current density i_d were determined.

2.6.3 Electrochemical Noise Measurements

Potential noise and current noise were recorded simultaneously using a control program developed by Mansfeld and Xiao [37-39]. For each measurement lasting 1024 seconds, a sampling rate of 2 points/second was used. Two identical samples with an exposed area of 5 cm^2 were placed vertically and parallel to each other in a test cell [37]. For data collection, 0 mV potential difference between the two samples was applied using a Schlumberger model 1286 potentiostat, a SCE was used as reference electrode.

The experimental noise data were processed using statistical analysis and simple spectral analysis as discussed in more detail by Mansfeld and Xiao [37-39]. The noise resistance R_n was determined as:

$$R_n = \sigma\{V(t)\}/\sigma\{I(t)\} \qquad\qquad [2\text{-}1]$$

where $\sigma\{V(t)\}$ is the standard deviation of potential fluctuations and $\sigma\{I(t)\}$ is the standard deviation of current fluctuations. The spectral noise response R_{sn} (f) was calculated at each frequency f as:

$$R(f) = V(f)/I(f) \qquad\qquad [2\text{-}2]$$

$$R_{sn}\ (f) = |R(f)| \qquad\qquad [2\text{-}3]$$

where V(f) and I(f) are complex numbers obtained from Fast Fourier Transformation (FFT). The spectral noise resistance R^o_{sn} was calculated as the dc limit of R_{sn} (f):

$$R^o_{sn} = \lim_{f \to 0} \{R_{sn}\ (f)\} \qquad\qquad [2\text{-}4]$$

2.7 Surface Analysis

Scanning Electron Microscopy (SEM), Energy Dispersive Spectroscopy (EDS) and elemental mapping were used for selected samples to obtain information concerning surface morphology, chemical composition and distribution of elemental components in the modified surfaces. The samples used for surface analysis included exposed and unexposed surfaces.

3. EXPERIMENTAL RESULTS

The corrosion behavior of Al and Al alloys exposed to 0.5 M NaCl was intensively investigated with electrochemical techniques such as EIS, polarization curve and electrochemical noise analysis. EIS measurements were employed to monitor the changes of surface properties during exposure, polarization curves were measured to determine the susceptibility of Al alloys to pitting in chloride containing environments and to reveal the mechanisms leading to improved resistance to localized corrosion for modified surfaces. Surface analyses using SEM, EDS, AES and elemental mapping were performed to obtain the information concerning surface morphology, chemical composition and element distribution for modified surfaces and determine the role of Ce and Mo in providing resistance to localized corrosion.

3.1 Localized Corrosion of Untreated Al Alloys

Localized corrosion in the form of pitting occurring on Al alloys exposed to 0.5 M NaCl (open to air) was intensively investigated to obtain a base line for evaluation of the corrosion behavior of modified surfaces. Pit initiation was determined both with EIS and by visual inspection, while continuous monitoring with EIS was performed to obtain insight into the pit propagation process. Quantitative analysis of EIS data was based on the pitting model [35,40-42] and led to derivation of pit growth laws for Al alloys exposed to NaCl.

3.1.1 Impedance Behavior

For Al alloys exposed to NaCl, localized corrosion in the form of pitting can be detected by EIS. Typical impedance behavior is shown in Fig. 4 for deoxidized Al 2024 during exposure to NaCl for 7 days. The occurrence of pitting corrosion detected by impedance spectra was characterized by a transmission line impedance at low frequencies for $f < 1$ Hz, which is an impedance with a constant slope between -0.5 and -1. A second time constant in the phase angle plot is apparent in the corresponding frequency range, which is sensitive indicator of pitting corrosion [40-42]. With increasing exposure time, pronounced decrease of impedance at intermediate frequencies and large increase of phase angle at lower frequencies were indicative of pit propagation process. Very similar spectra were obtained for as-received Al 6061 and Al 7075 exposed to the same environment (Fig. 5 and 6).

Pit initiation was observed for as-received Al 6061 in less than one day and for Al 7075 and in less than 2 hours for Al 2024 which was very susceptible to pitting. The pit growth rates on these three commercial Al alloys at E_{corr} were determined from the specific polarization resistance of the pitted surface R^o_{pit} based on the EIS data collected as a function of time (Fig. 7). The relationship between pit growth rate expressed as $1/R^o_{pit}$ and time t can be described by the form:

$$\log (1/R^o_{pit}) = \log a + b \log t, \qquad\qquad [3\text{-}1]$$

where a and b are experimental parameters, a is found to depend on both alloy composition and surface condition, and b depends on the mechanism of pit propagation. Table VIII gives experimental values of log a and b obtained by fitting the data in Fig. 7 to Eq. 3-1. Since for all three alloys b is nearly close to -1 (Table VIII), it can be assumed that the pit growth law follows the general equation

$$dr/dt = a' \, t^{-1} \qquad\qquad [3\text{-}2]$$

Table VIII. Values of log a and b for pitting process of Al alloys

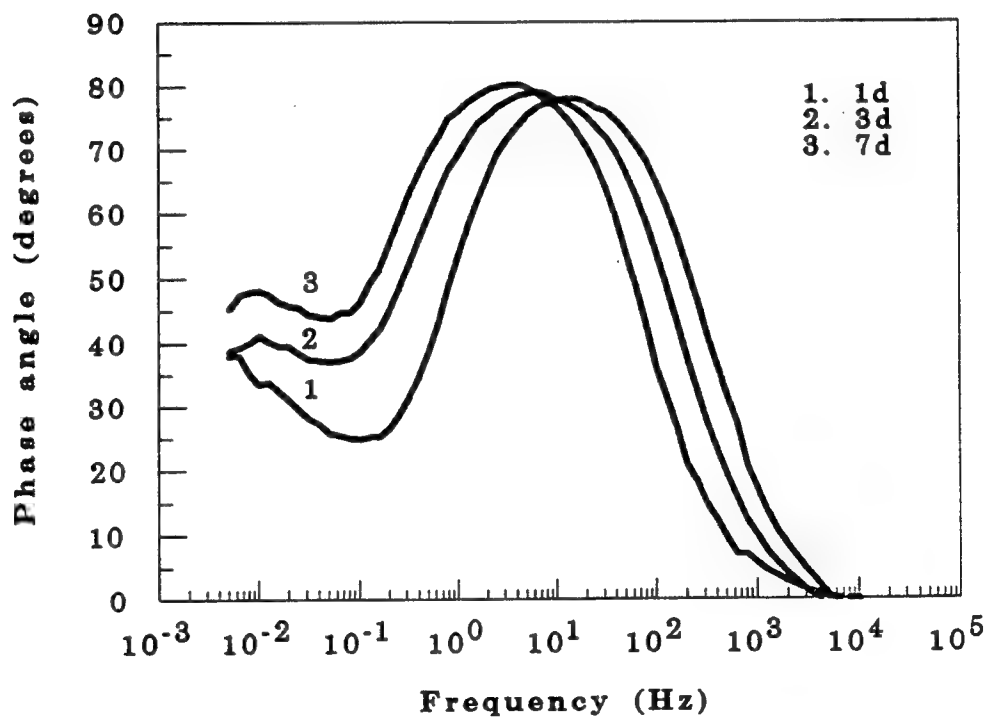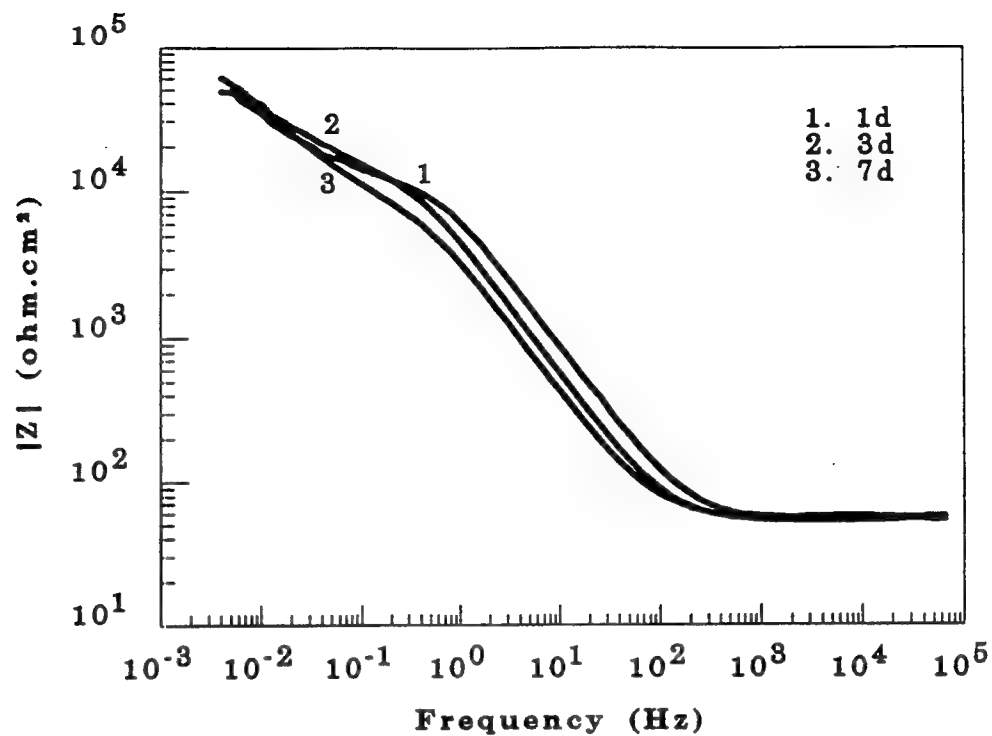| Alloys	log a	b
Al 2024/deoxidized	-2.24	-0.82
Al 6061/as-received	-1.77	-1.34
Al 7075/as-received	-1.85	-1.38

Fig. 4. Impedance spectra for Al 2024/deoxidized as a function of exposure time to 0.5 M NaCl
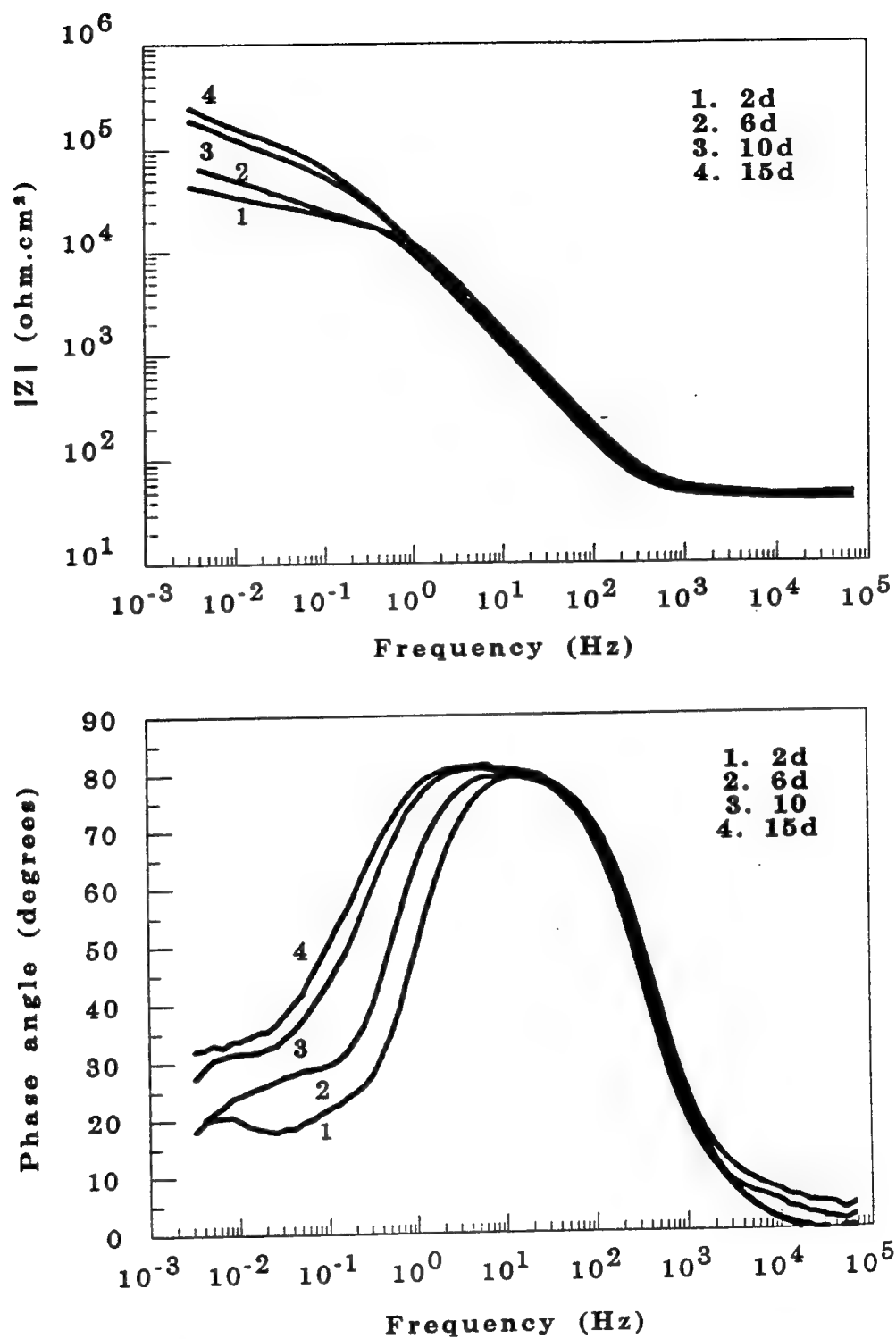
Fig. 5. Impedance spectra for Al 6061/as-received as a function of exposure time to 0.5 M NaCl
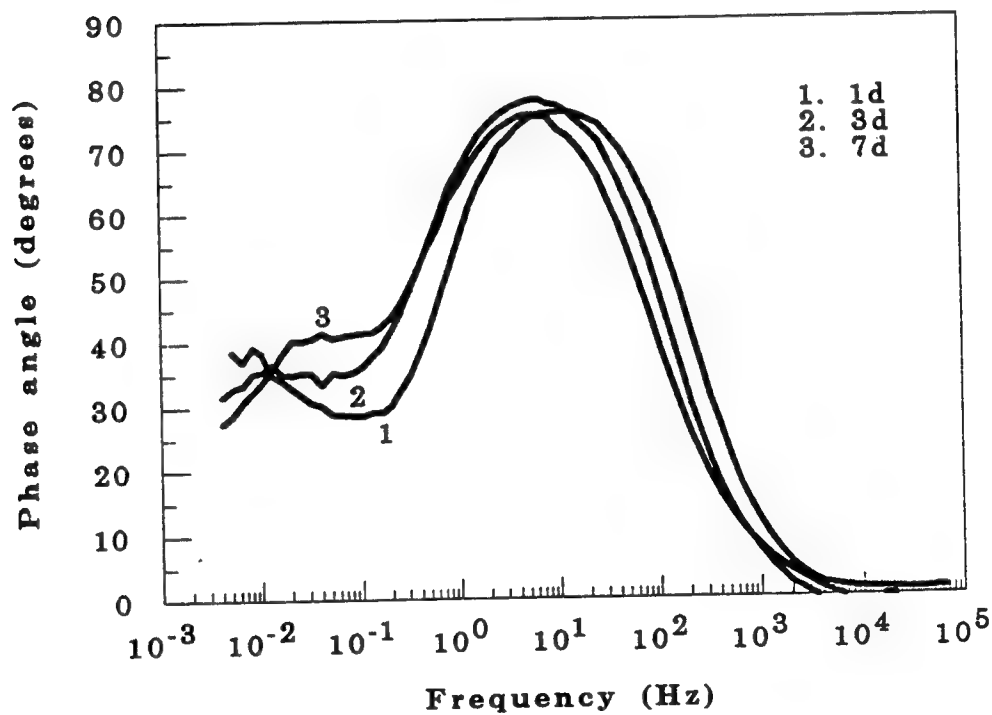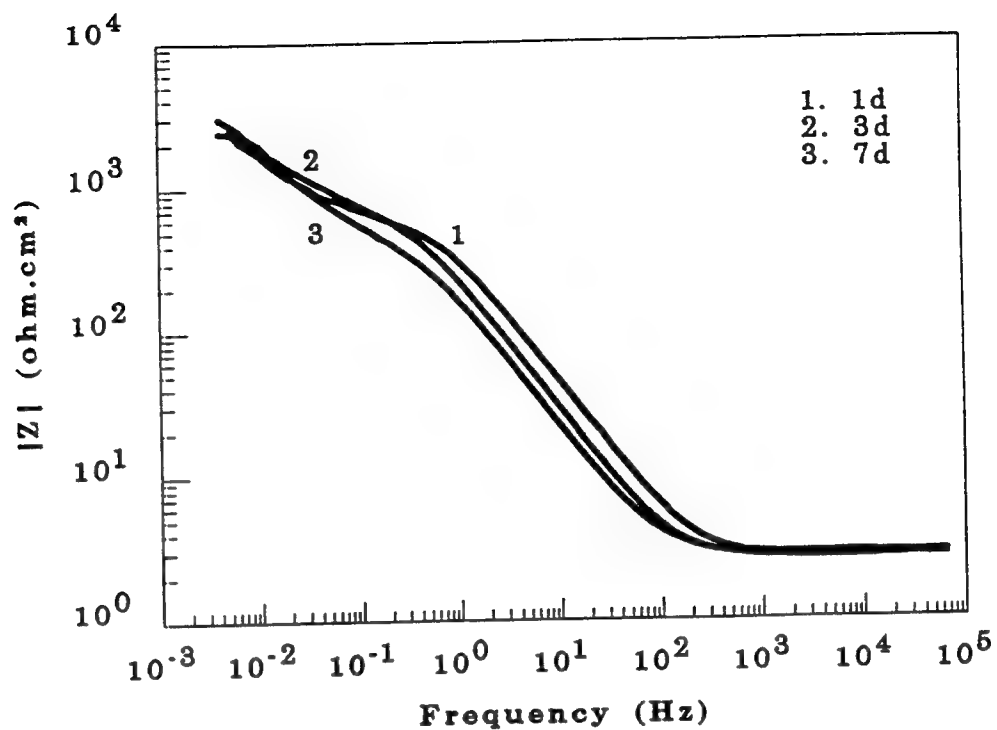
Fig. 6. Impedance spectra for Al 7075/as-received as a function of exposure time to 0.5 M NaCl
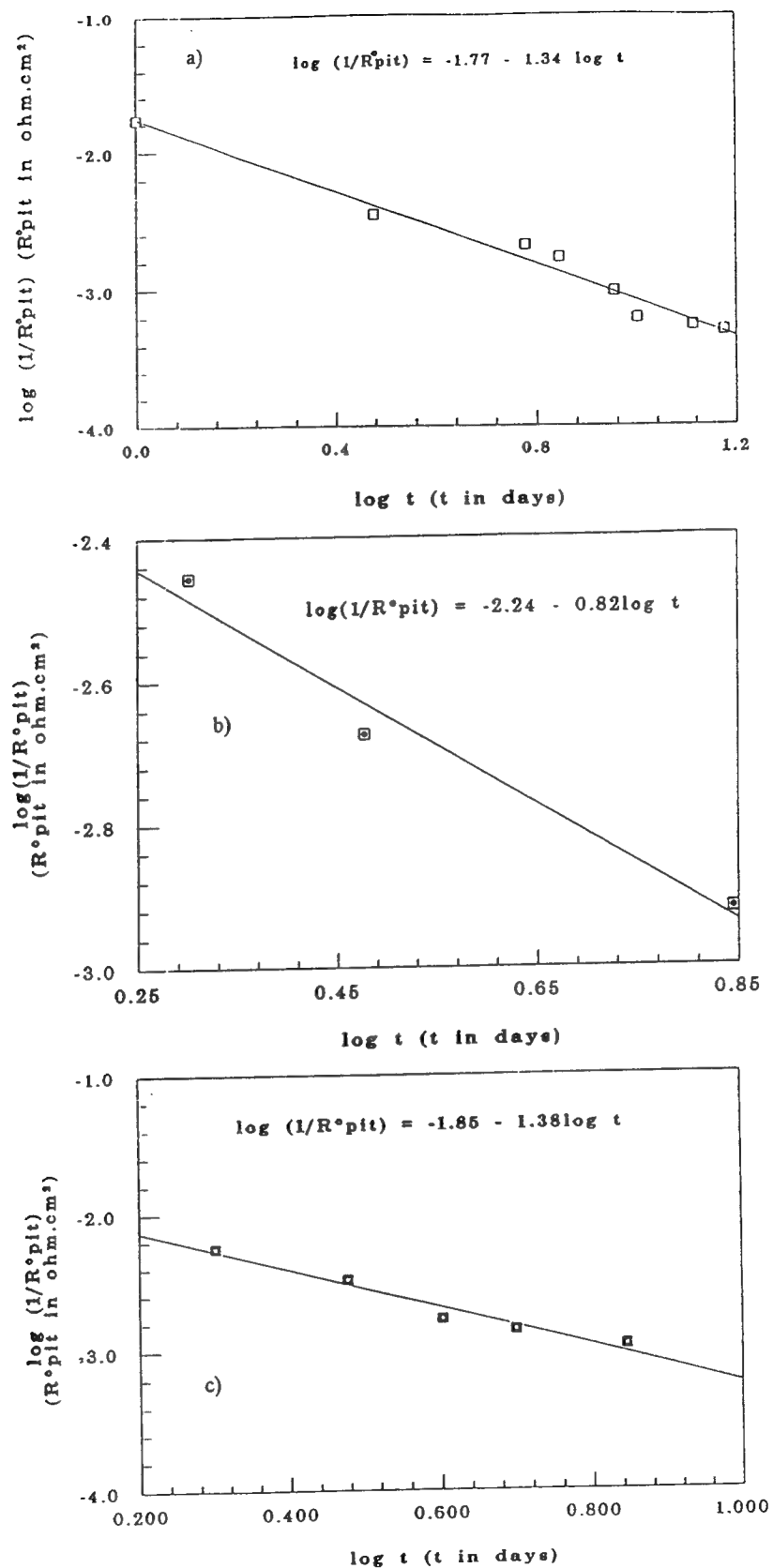
Fig. 7. Plots of log (1/R⁰pit) vs log t for Al alloys exposed to 0.5 M NaCl
a) Al 6061/as-received, b) Al 2024/deoxidized, c) Al 7075/as-received

which suggests that for hemispherical pits the pit radius r increases logarithmically with time as:

$$r = a' \log (t_p/t_o) \hspace{4cm} [3\text{-}3]$$

In Eq. [3-3] $t_p > t_o$ with t_o being the time at which pits were first observed. The parameter a' can be defined as the pit growth rate at $t = 1$.

3.1.2 Polarization Curves

Anodic polarization curves for deoxidized Al 2024-T3, as-received Al 6061-T6 and Al 7075-T6 were measured in 0.5 M NaCl (open to air). The results are shown in Fig. 8. For these three Al alloys, when polarized anodically, pits were generated immediately and the current increased sharply with anodic polarization. At higher anodic potentials polarization curves displayed ohmic controlled behavior and no passive region existed. E_{pit} and E_{corr} were found to be identical for these untreated alloys. The experimental values of E_{pit} and E_{corr} determined from the polarization curve are summarized in Table IX.

3.2 Surface Modification of Low-Cu Al Alloys

For Al 6061, Al 6013 and pure Al surface modification consisted of immersion in boiling 10 mM $Ce(NO_3)_3$ for 2 hours, in boiling 5 mM $CeCl_3$ for 2 hours at 100°C, and anodic polarization in 0.1 M Na_2MoO_4 at +500 mV vs. SCE for 2 hours at room temperature (Table V). Before surface modification, samples were deoxidized in Diversey 560 at room temperature for 10 minutes, and then baked in an oven at 100°C for at least 24 hours to grow a new, reproducible aluminum oxide film. In earlier experiments, the Na_2MoO_4 solution was deaerated for 2 hours prior to the polarization and a SCE was used as the reference electrode during the treatment in 0.1M Na_2MoO_4.

3.2.1 Impedance Behavior of Surface Modified Al 6061

In Fig. 9, impedance spectra are shown for surface modified Al 6061 as a function of exposure time to 0.5 M NaCl. A comparison of the EIS data obtained after 1 day for untreated and modified samples is plotted in Fig. 10. For modified Al 6061, impedance spectra were capacitive and remained unchanged for a period of 30 days. These features indicate that uniform corrosion was very low and localized corrosion did not occur. As shown before, EIS is very sensitive to the occurrence of localized corrosion on Al alloys. For untreated Al 6061, pit initiation was detected by occurrence of a transmission line impedance and a second time constant in the phase angle plot in the lower frequency region after only 1 day of exposure to 0.5 M NaCl (Fig. 4 - 6). This comparison illustrates the remarkable improvements in the corrosion resistance achieved by the Ce-Mo process.

More detailed information concerning corrosion behavior for the modified surface can be obtained from plots of R^o_p and C^o_p as a function of time. As shown in Fig. 11, R^o_p remained close to 10^7 ohm.cm^2 during the entire test period corresponding to very low corrosion rates. C^o_p was about 3.4 µF/cm^2. The constant values of R^o_p and C^o_p reflect the excellent stability of the modified surface in an aggressive solution. These results are in agreement with visual observation which showed an uncorroded surface for modified sample after exposure to 0.5 M NaCl for 30 days.

Table IX. E_{corr} and E_{pit} for Al alloys exposed to 0.5 M NaCl

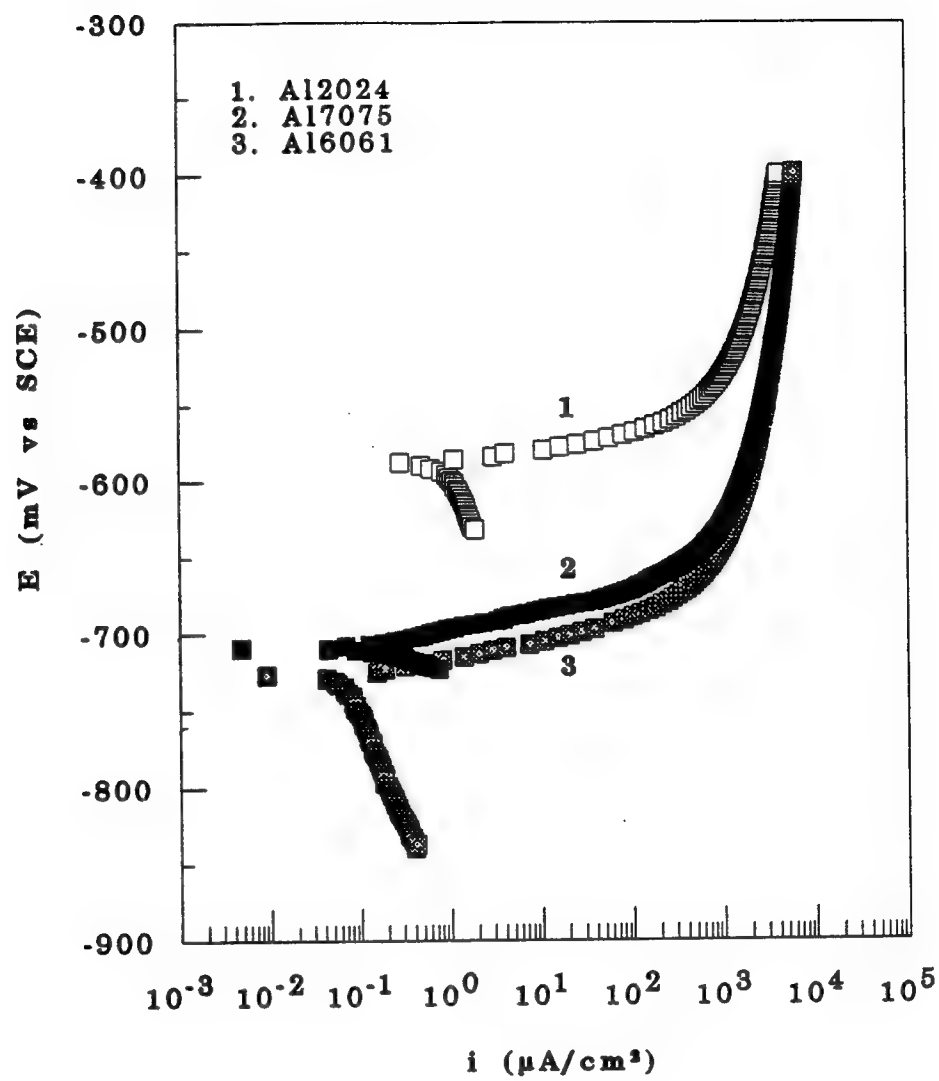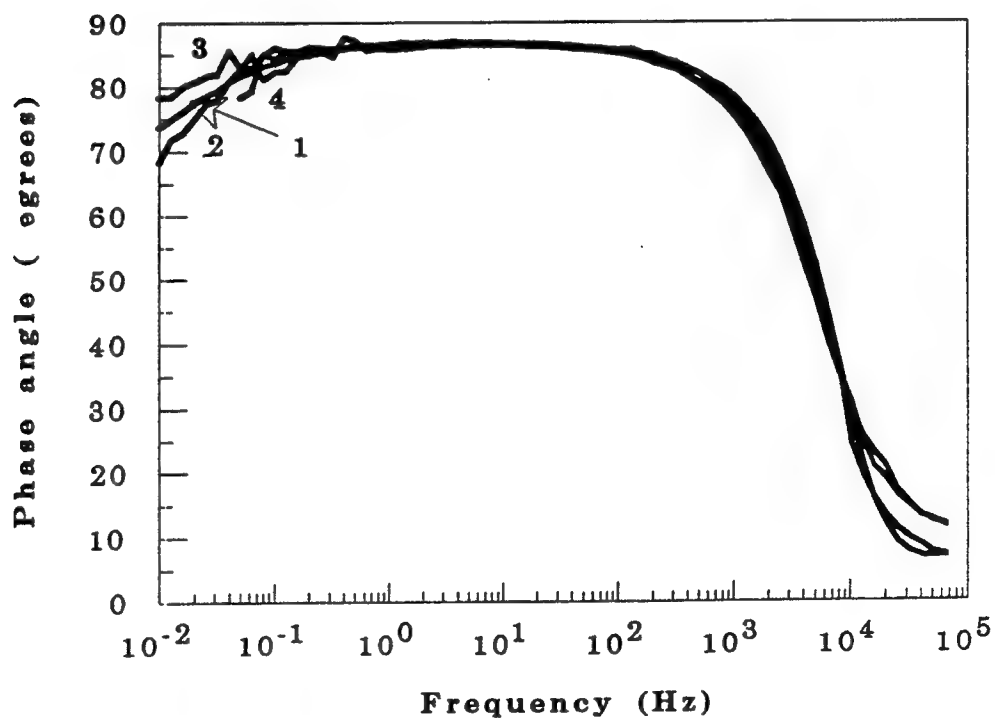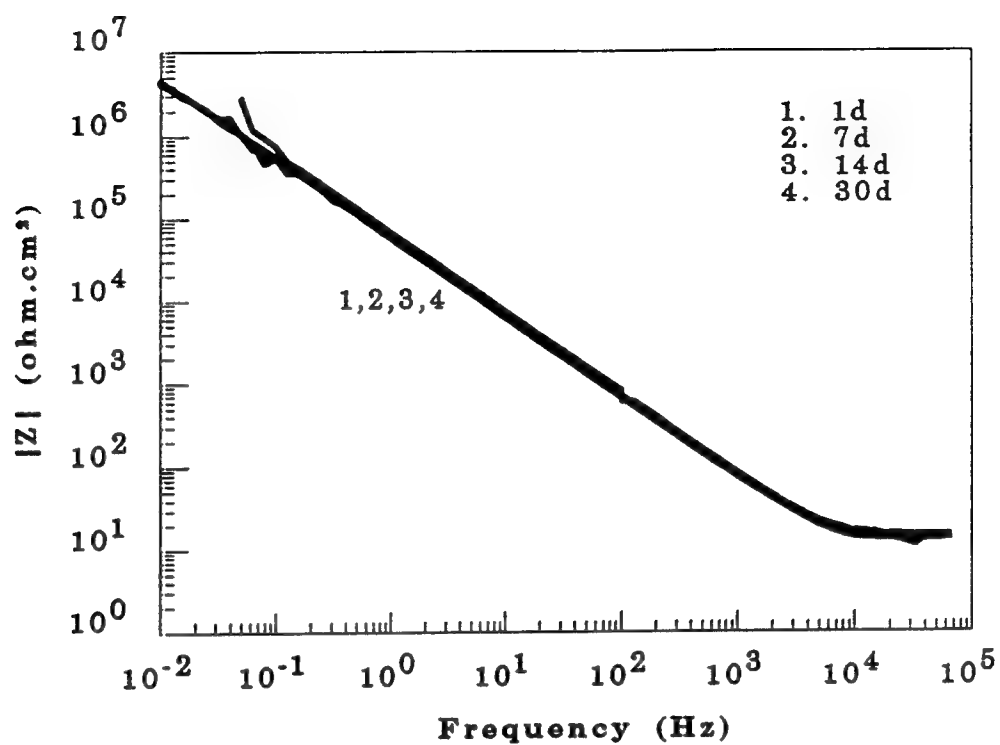| Alloys	E_{corr} (mV vs. SCE)	E_{pit} (mV vs. SCE)
Al 2024/deoxidized	-588	-588
Al 6061/as-received	-725	-725
Al 7075/as-received	-710	-710

Fig. 8. Polarization curves for Al alloys in 0.5 M NaCl

Fig. 9. Impedance spectra for Al 6061/Ce-Mo process as a function of exposure time to 0.5 M NaCl
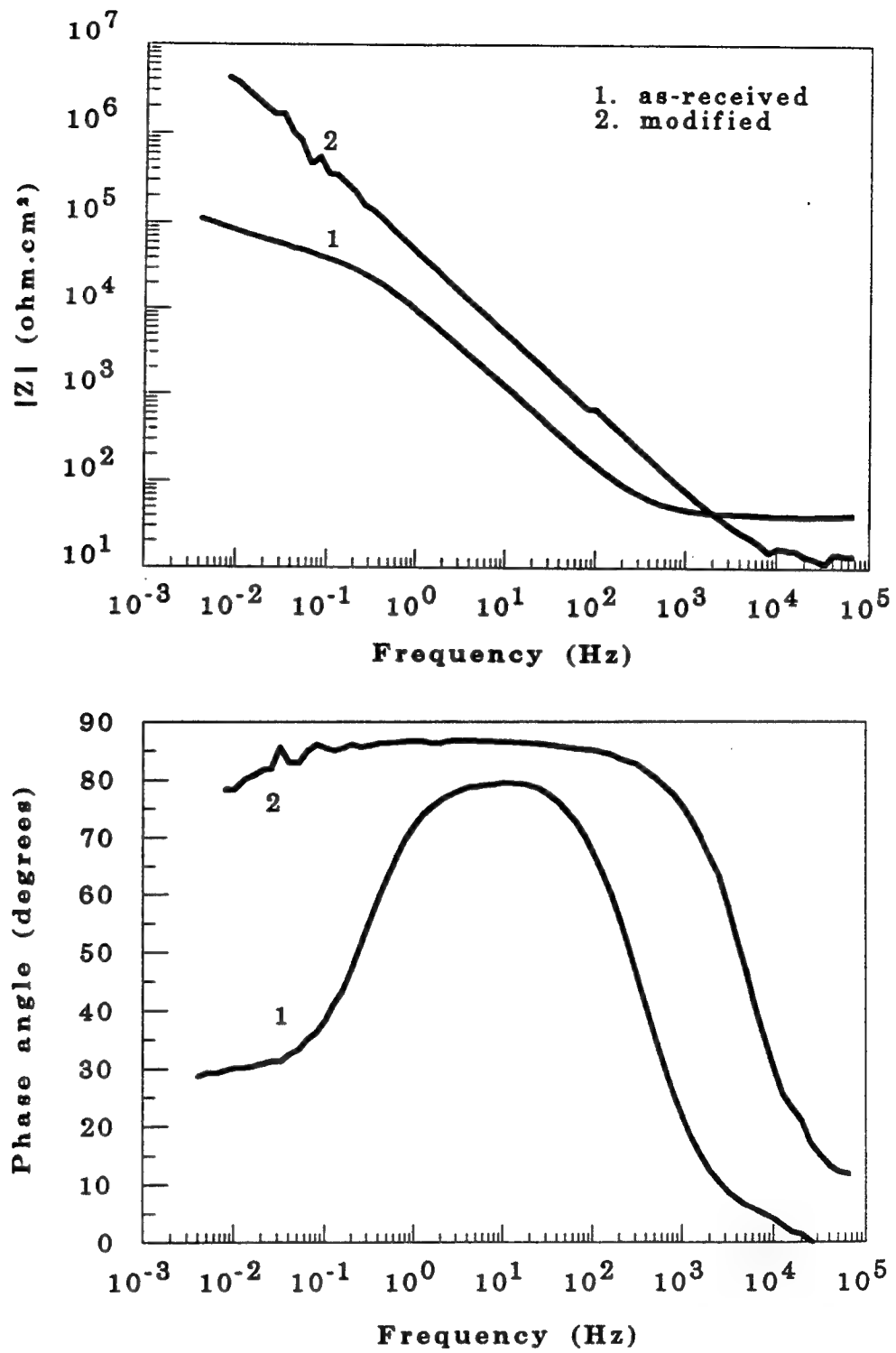
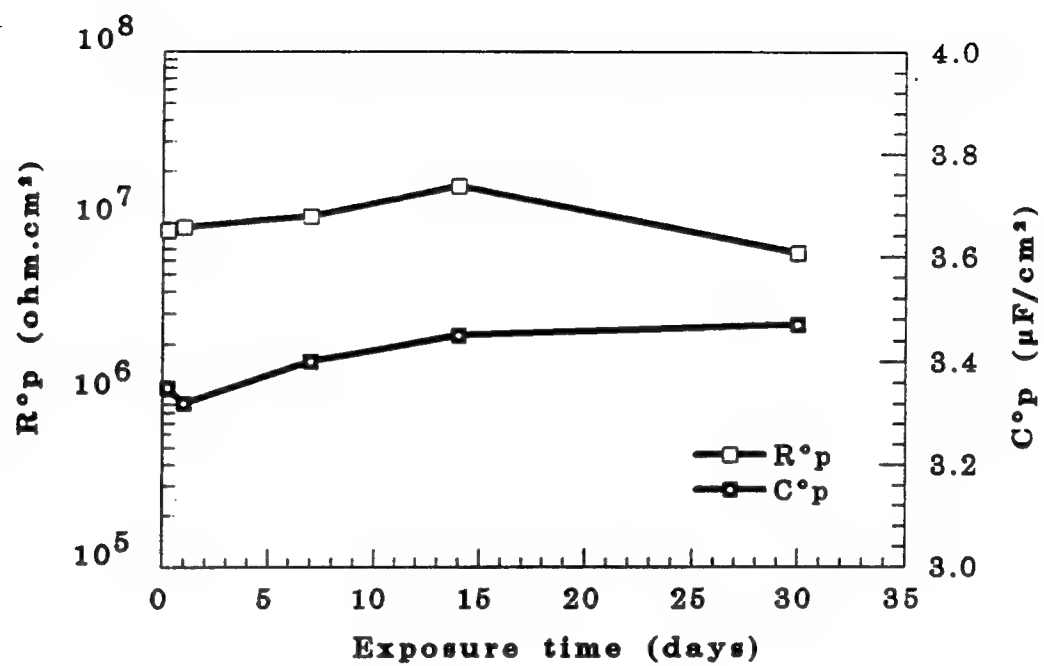Fig. 10. Comparison of EIS data for untreated and modified Al 6061

Fig. 11. R^o_p and C^o_p for Al 6061/Ce-Mo process as a function of exposure time

3.2.2 Polarization Behavior

Polarization curves were measured to determine the mechanism by which the surface modification increases corrosion resistance. In Fig. 12, curve 1 shows anodic polarization behavior for untreated Al 6061 in 0.5 M NaCl, for which E_{corr} and E_{pit} (-708 mV vs. SCE) coincide. Dramatic changes of the polarization curve were observed for the modified sample. E_{corr} had shifted to -485 mV and E_{pit} was about -325 mV, while i_p was less than 0.003 $\mu A/cm^2$ (curve 2). This value of i_p is much lower than $i_p = 1$ $\mu A/cm^2$ for SS 304 in 0.5 M NaCl, and orders of magnitude lower than that in deaerated 1000 ppm NaCl for pure Al sputter-deposited onto Si single-crystal and passivated by anodic polarization in Na_2MoO_4 solution [29].

The unique properties of modified surfaces can be illustrated by the anodic polarization curve after immersion in NaCl for one month. As shown in Fig. 13, E_{corr} was about -690 mV and E_{pit} had shifted to -534 mV. However, the difference between E_{corr} and E_{pit} had not changed (see Fig. 12 and 13). Starting at E_{corr}, a very small i_p in the nA/cm^2 range was recorded, which was below the detection limit of the potentiostat. When E_{pit} was reached, the current increased and a polarization curve with an active-passive transition followed by a constant current region was obtained, where the current density was 3 $\mu A/cm^2$. After the polarization test, the sample surface was examined by SEM. Only a few pits with small dimensions had developed, while the remainder of the surface was completely unattacked. Apparently, the polarization curve in Fig. 13 represents that of these single pits.

Recording of cathodic polarization curves in 0.5 M NaCl showed that the rate of the oxygen reduction reaction was reduced on the modified surfaces (Fig. 14). The current density at -850 (mV vs SCE) was 0.08 $\mu A/cm^2$ for the modified surface, while at the same potential the current density for the untreated sample was 1.5 $\mu A/cm^2$. Apparently, the modified surface does not allow either oxidation or reduction processes to occur at appreciable rates and showed behavior typical of an insulator.

3.2.3 Role of Process Parameters

The Ce-Mo process has produced very corrosion resistant surfaces on Al alloys. In order to evaluate the effects of boiling and anodic polarization and to understand the roles of Ce and Mo in the Ce-Mo process (Table V), three samples of Al 6061 with different surface treatments were prepared. Sample A was prepared using the Ce-Mo process, sample B was polarized in borate buffer solution instead of polarization in Na_2MoO_4 after treating in Ce solutions, while sample C was treated in boiling distilled water, followed by anodic polarization in Na_2MoO_4.

The corrosion behavior for these three samples was evaluated in 0.5 M NaCl by collecting EIS data continuously for at least 15 days. Comparison of EIS data is shown in Fig. 15 for one day and Fig. 16 for 15 days. The spectra for sample A remained totally capacitive (curve A), while for the other two samples, EIS data for one day showed a deviation behavior from capacitive spectra and became typical of localized corrosion with increasing exposure time, which was indicated by transmission line impedance and a second time constant in the low frequency region (Fig. 16). Pit initiation was visually observed after 5 days for sample B and after 2 days for sample C.

Analyses of the EIS data provides electrochemical parameters which can be used to evaluate
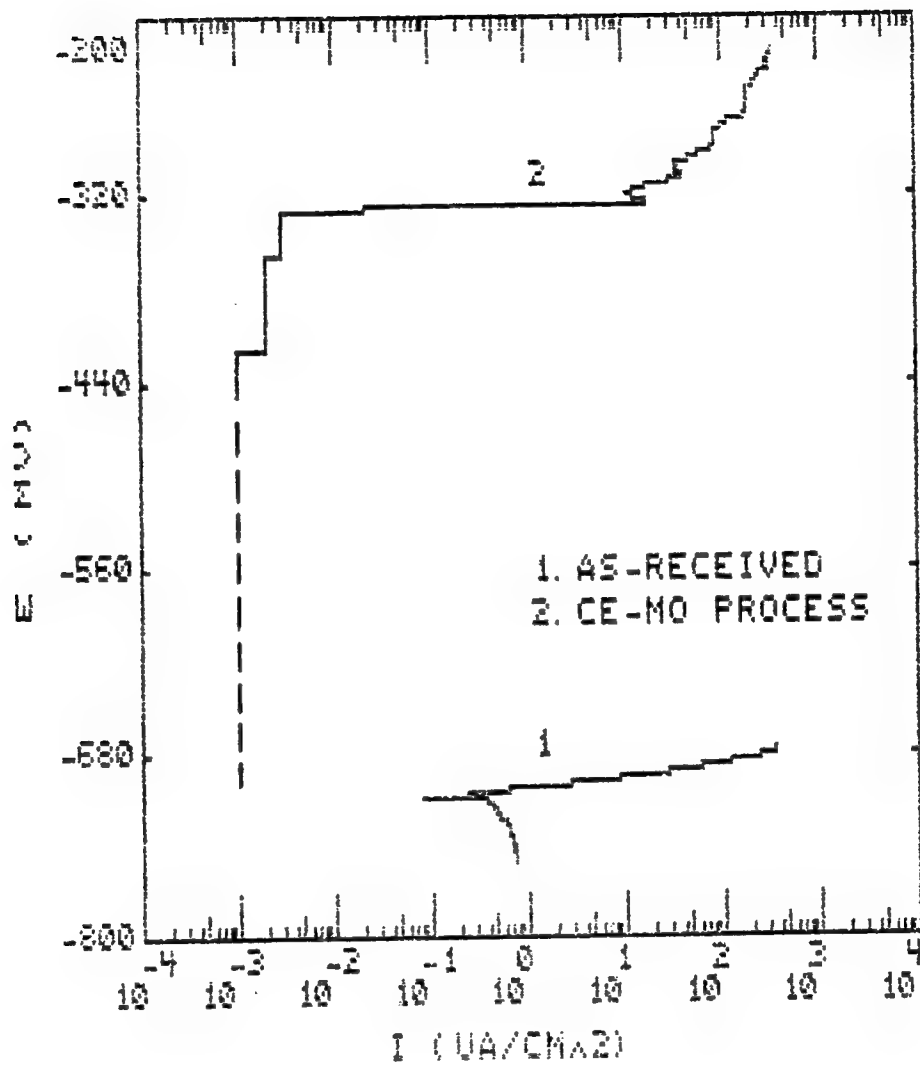
-23-

Fig. 12. Anodic polarization curves for Al 6061 (as-received vs modified) in 0.5 M NaCl; 1) as-received, 2) modified in the Ce-Mo process
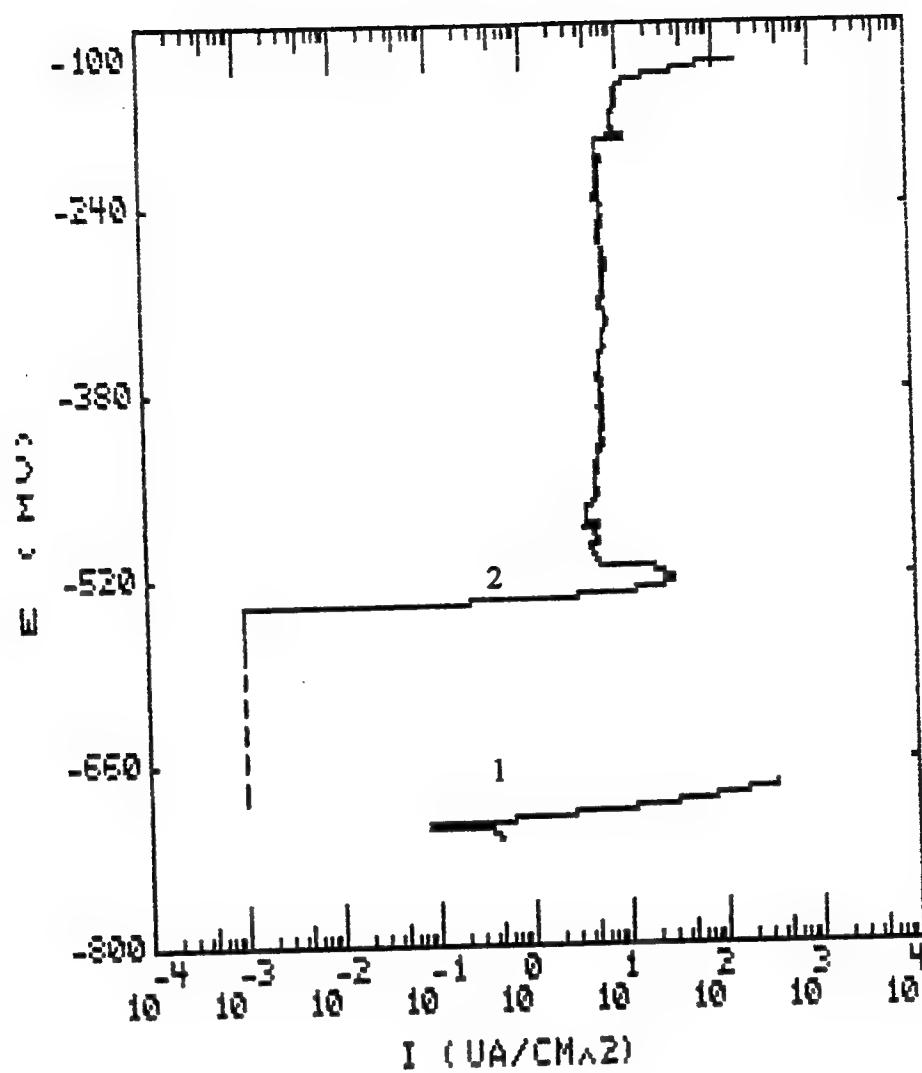
Fig. 13. Anodic polarization curves for Al 6061 (as-received vs modified) in 0.5 M NaCl; 1) as-received, after 2 hours, 2) modified by the Ce-Mo process, after 30 days
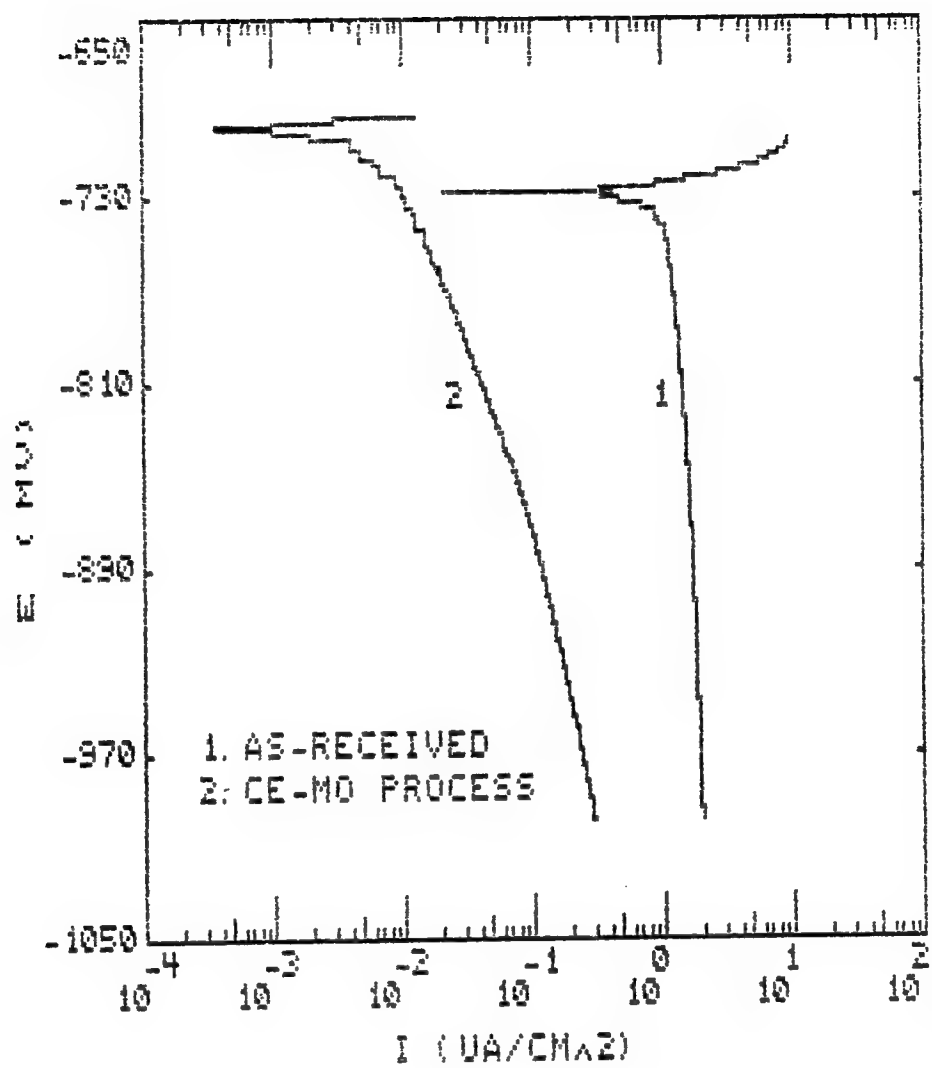
Fig. 14. Cathodic polarization curves for as-received vs modified Al 6061 in 0.5 M NaCl; 1) as-received, 2) modified in the Ce-Mo process
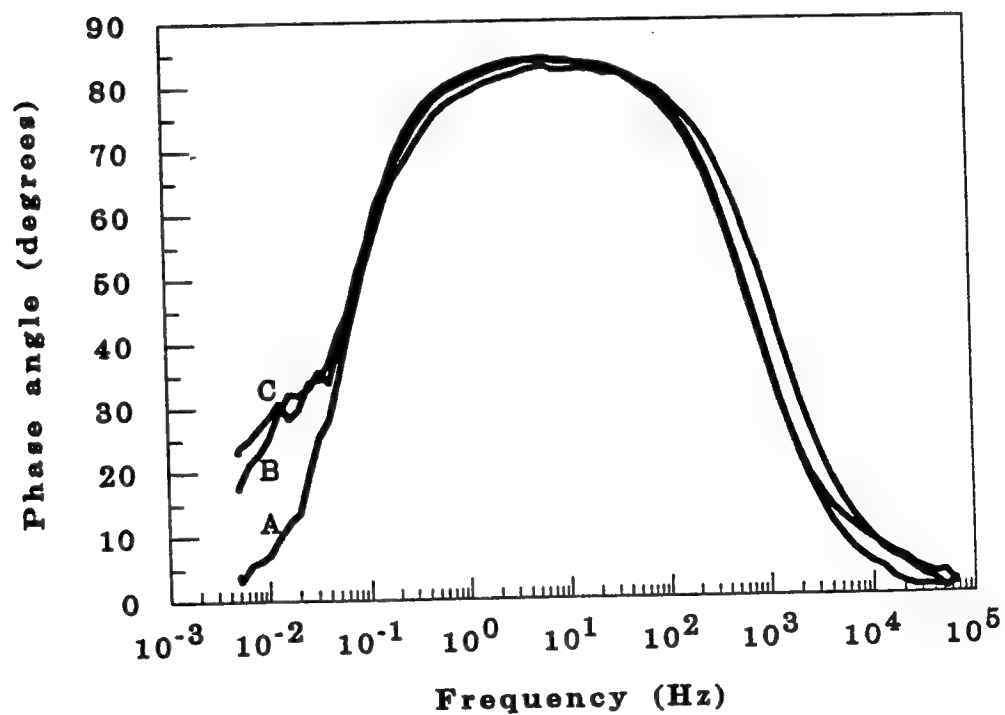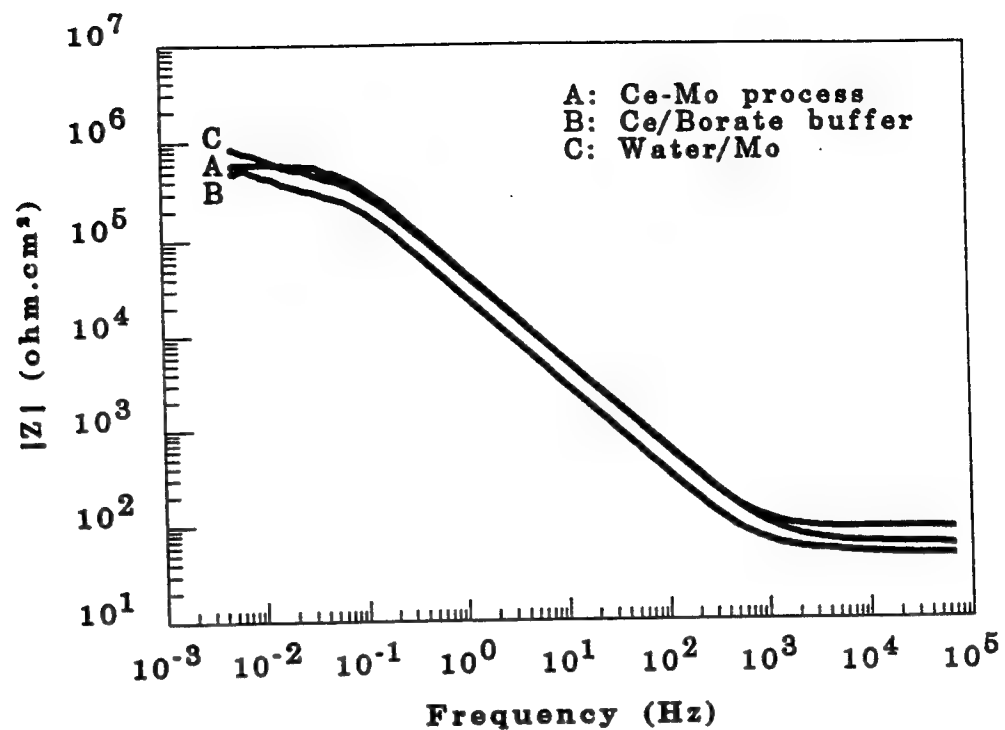
Fig. 15. Comparison of impedance spectra for Al 6061 with different treatments exposed to 0.5 M NaCl for 1 day
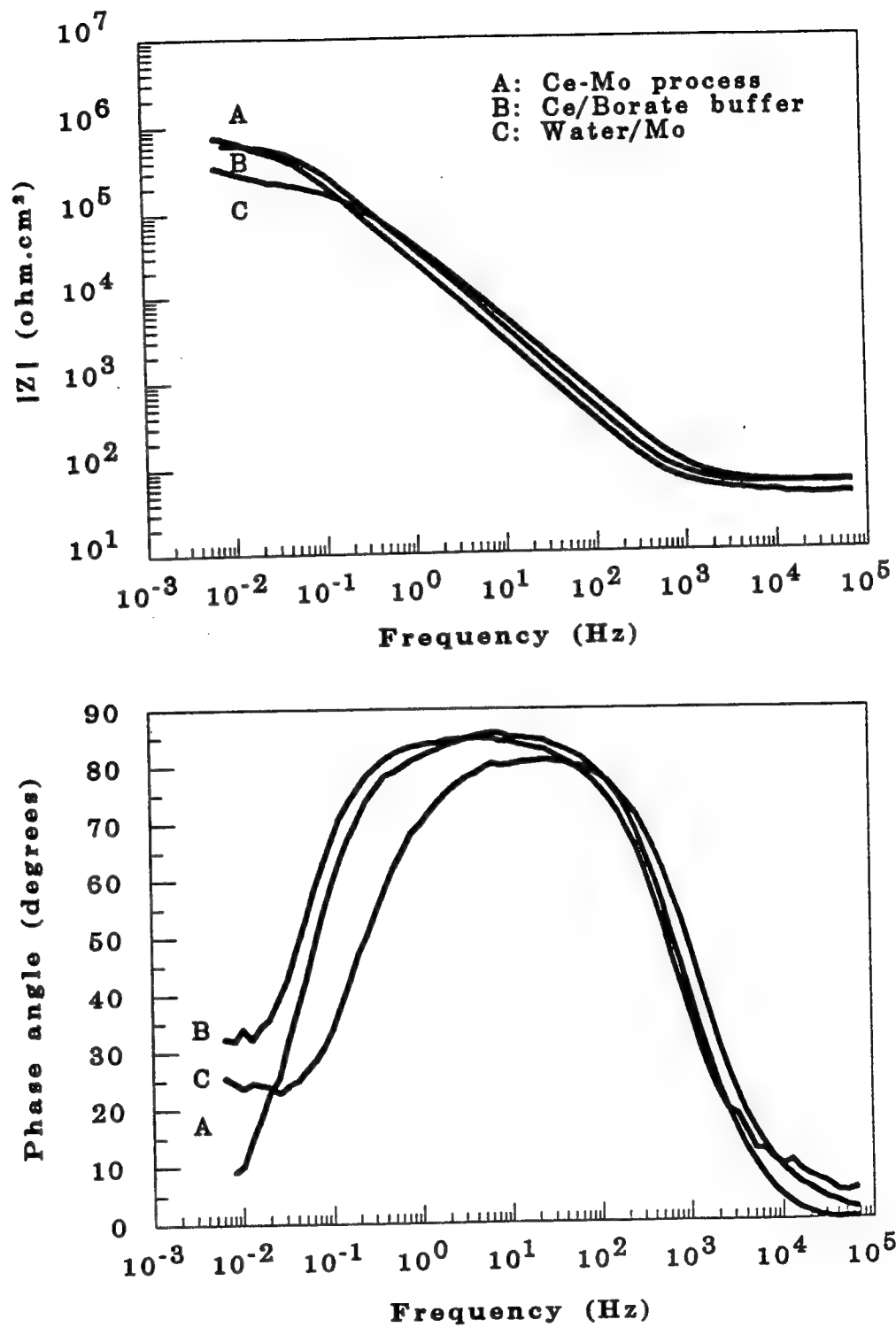
Fig. 16. Comparison of impedance spectra for Al 6061 with different treatments exposed to 0.5 M NaCl for 15 days

the corrosion behavior of these three different surfaces. Sample A had the smallest capacitance C^o_p and the highest R^o_p as shown in Fig. 17 and 18. Pit growth rates estimated from R^o_{pit} were slightly lower for sample B than for sample C (Fig. 19). These results suggest that neither boiling in hot water or polarization in borate buffer solution produces corrosion resistant surface on Al alloys. Apparently the excellent corrosion resistance of the modified surface layers is due to synergistic effects between Ce and Mo. Boiling in hot water seems to increase the thickness of the surface oxide layer corresponding to lower value of C_t. Polarization in borate buffer solution increases pitting resistance marginally as indicated by increased pitting time.

3.2.4   Surface Analysis

The result of EDS analysis indicated the presence of both Ce and Mo in the modified surface layers (Fig. 20). Peaks were detected for Ce at 5.02 keV and for Mo at 2.30 keV. For a modified sample which had been exposed to NaCl for 30 days, chemical composition profiles obtained by AES showed Ce to be present in fairly large amounts in the modified surface layers, while the concentration of Mo was apparently low (Fig. 21). It is possible that Mo did not precipitate uniformly over the surface, with most of the incorporated Mo being located at sites where anodic dissolution occurred as will be discussed below.

3.2.5   Surface Modified Pure Aluminum

For pure Al (99.99%), very corrosion resistant surfaces were produced by the Ce-Mo process. EIS data for a modified sample exposed to NaCl are shown in Fig. 22. The impedance spectra did not show any changes for 28 days, the transmission line type of impedance which occurred to untreated pure aluminum at the lower frequencies (Fig. 1 - 3) was not detected. For the spectra in Fig. 22 a capacitive feature was dominant, although the impedance spectra displayed a deviation from those for passive surface at low frequencies. This deviation is considered to be due to surface roughness since such behavior was not measured for a polished surface exposed to the same solution after 2 days (Fig. 23). Fig. 24 shows the time dependence of R^o_p and C^o_p for the modified surface, which were obtained by fitting the EIS data in Fig. 22 to the EC shown in Fig. 2. R^o_p was approximately constant at about 10^6 ohm.cm^2, while C^o_p increased slightly from 11 μF/cm^2 to 13 μF/cm^2 during exposure.

The effect of mechanical damage to surface modified pure Al was evaluated by making a deep scratch on the surface. Fig. 25 shows impedance spectra as a function of time for the scratched sample exposed to 0.5 M NaCl. Unchanged impedance spectra during prolonged exposure could be an indication of the passive nature of the modified surface because decreased impedance and increased phase angle typical of the pitting process were not detected. Observation of the sample surface by SEM at the end of the tests did not show evidence of general or localized corrosion in the scratched area (Fig. 26). Since localized corrosion did not occur, it has to be assumed that the occurrence of the transmission line impedance at f < 1 Hz (Fig. 25) is caused by the deep scratch and reflects geometric effects rather than localized corrosion phenomena.

3.2.6   Surface Modified Al 6013

Surface modification of Al 6013 in the Ce-Mo process was also performed to increase its pitting resistance. In Fig. 27, EIS data for the modified surface are compared with the impedance spectra for untreated Al 6013. Significant differences between these spectra were observed. For the untreated sample, the occurrence of pitting corrosion indicated by a transmission line
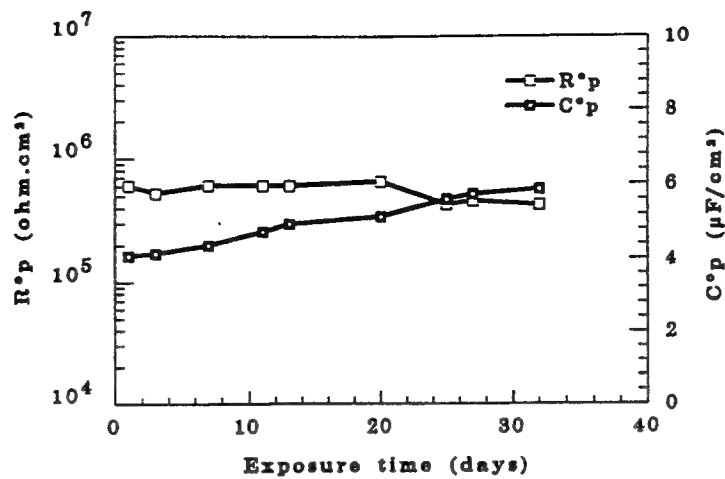
Fig. 17. R^o_p and C^o_p for Al 6061/Ce-Mo process as function of exposure time
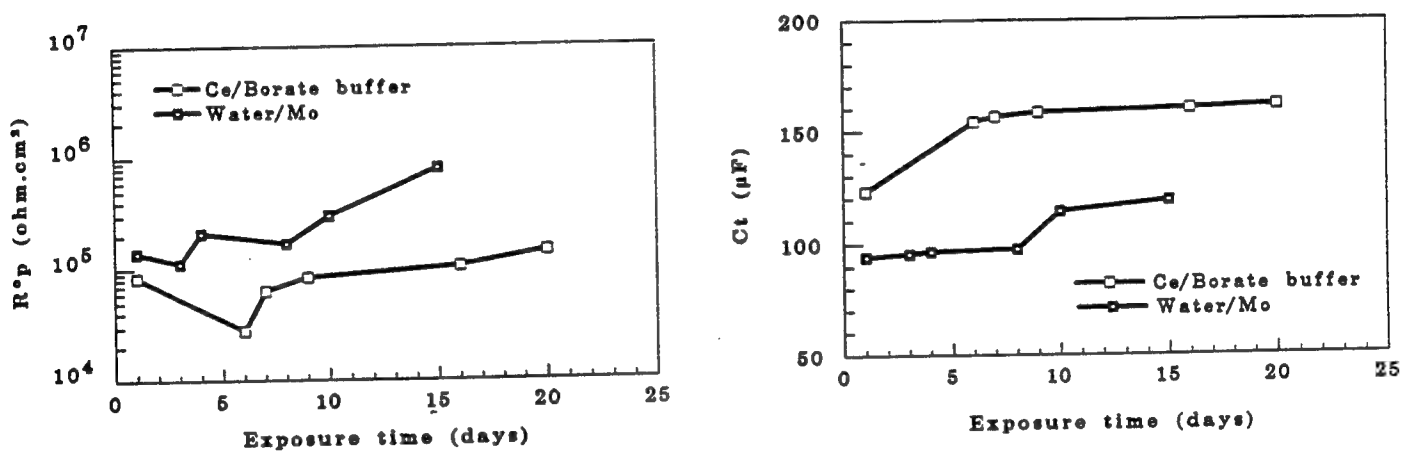

Fig. 18. R^o_p and C_t for Al 6061 with different treatments as function of exposure time
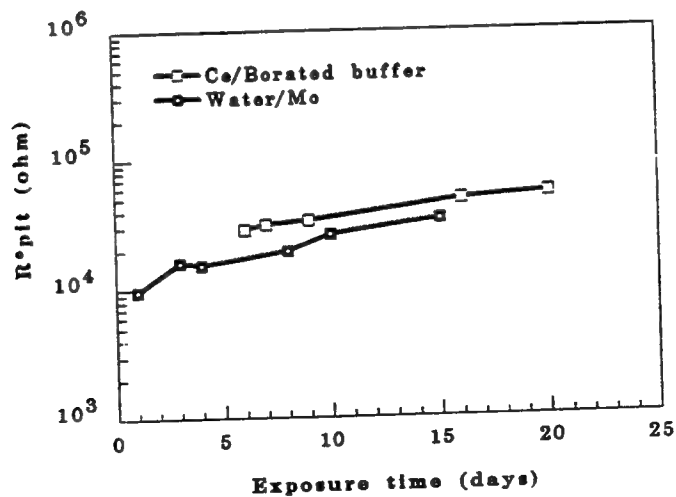

Fig. 19. R^o_{pit} for Al 6061 with different treatments as function of exposure time to 0.5 M NaCl
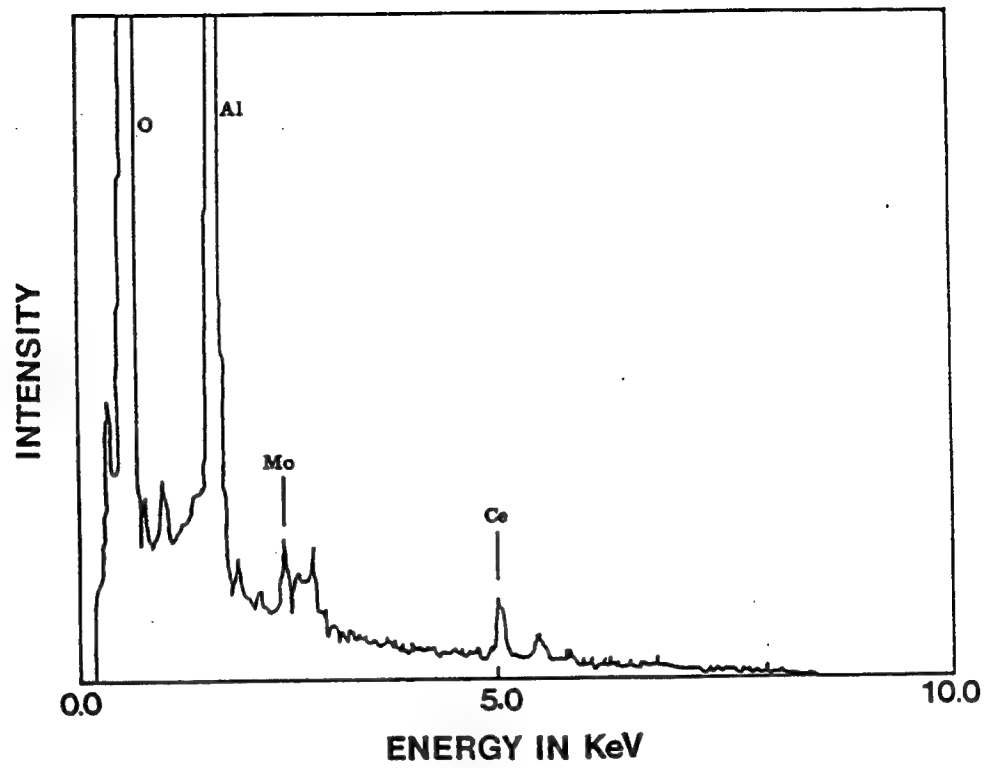
Fig. 20. Results of EDS analysis for Al 6061 modified in the Ce-Mo process
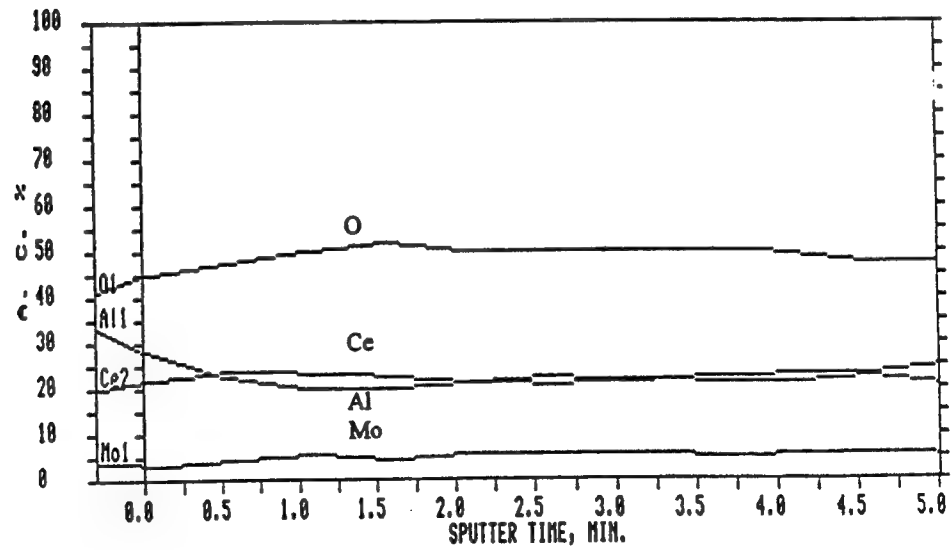
Fig. 21. AES concentration profile for Al 6061 modified in the Ce-Mo process
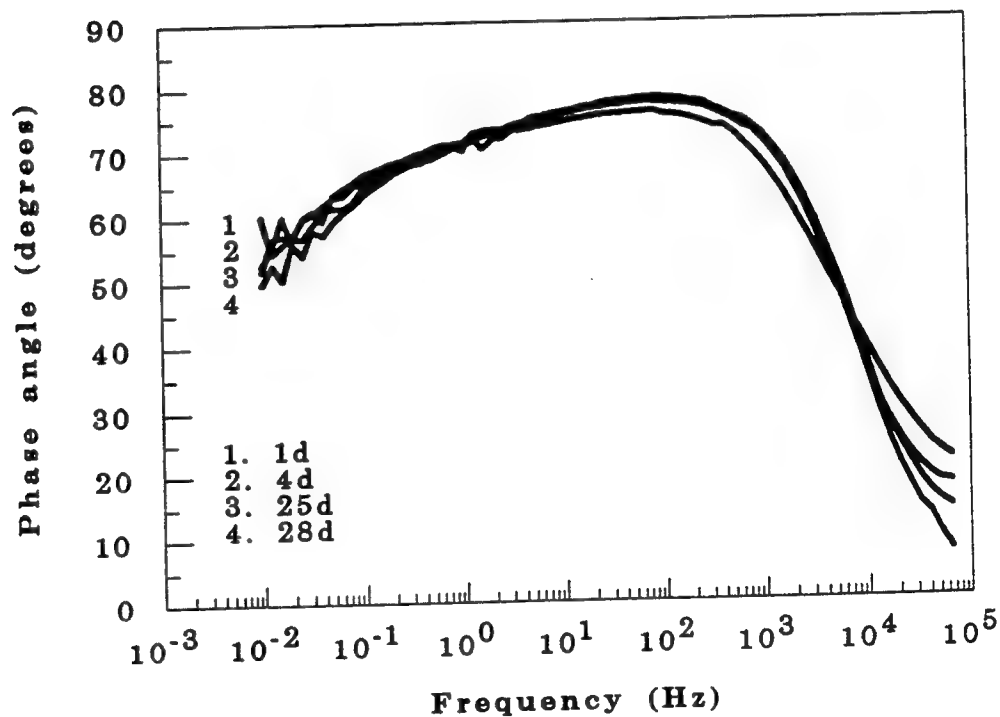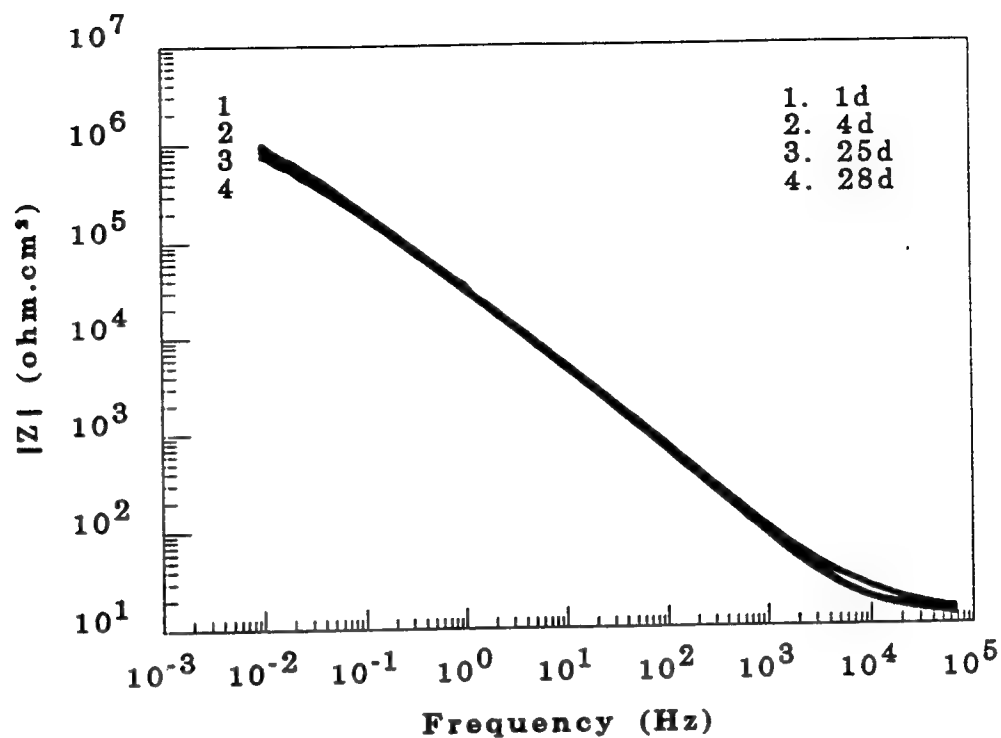
Fig. 22. Impedance spectra for pure Al/Ce-Mo process as a function of exposure time to 0.5 M NaCl
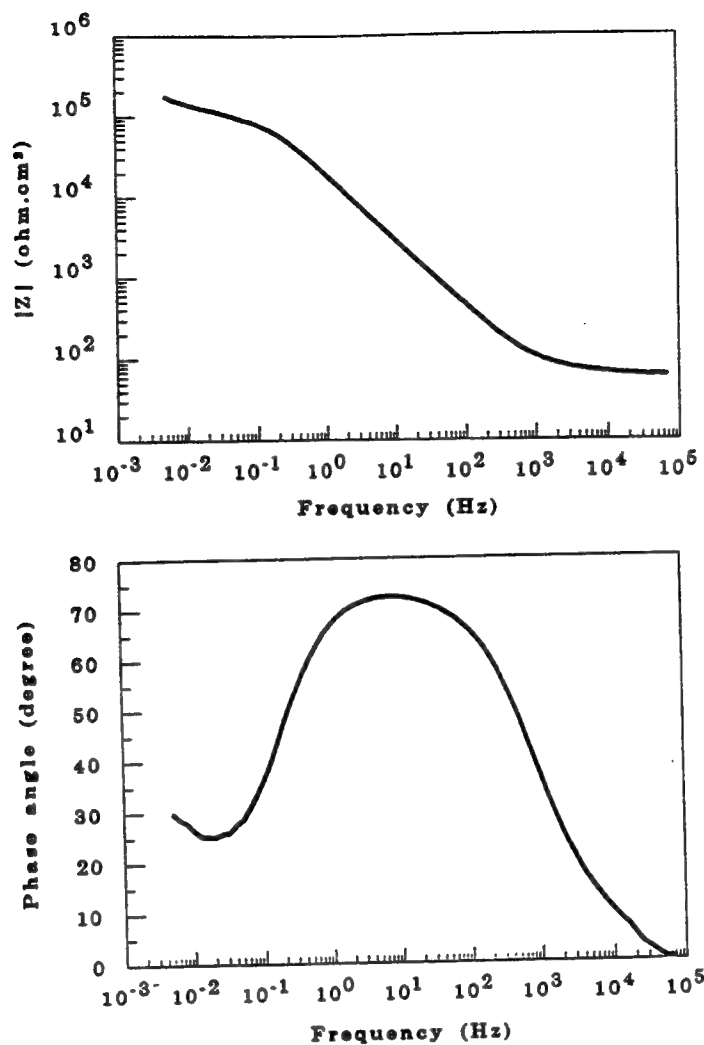
Fig. 23. Impedance spectra for pure Al/polished as a function of exposure time to 0.5 M NaCl for 2 days

Fig. 24. R^o_p and C^o_p for pure Al/Ce-Mo process as function of exposure time

Fig. 25. Impedance spectra for pure Al/Ce-Mo process with a scratch as a function of exposure time to 0.5 M NaCl

Fig. 26.   Scratched surface after 25 days of exposure to 0.5 M NaCl

Fig. 27. Comparison of impedance spectra for Al 6013 (as-received vs. surface modified)
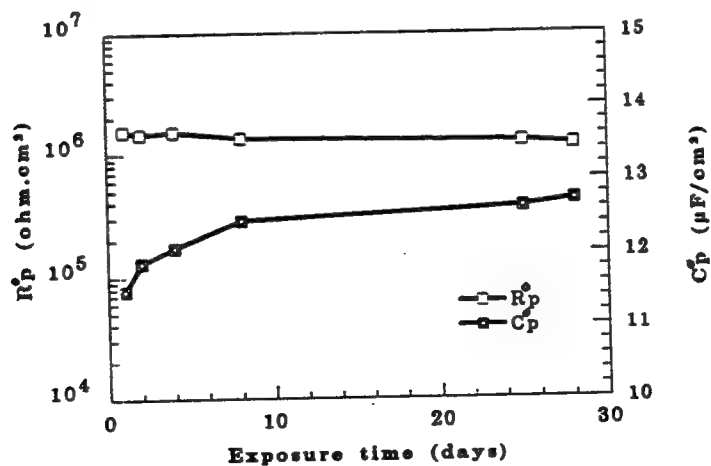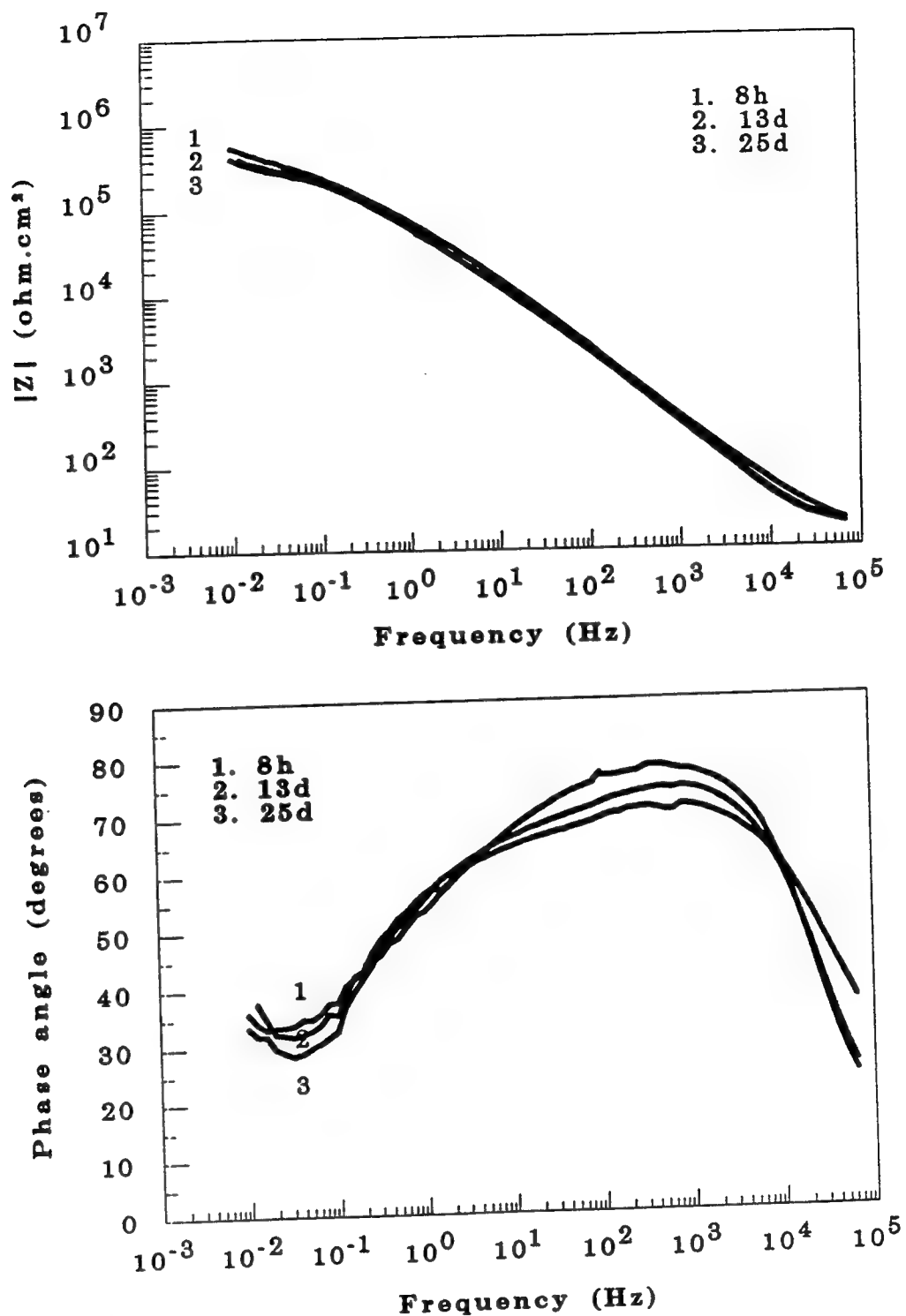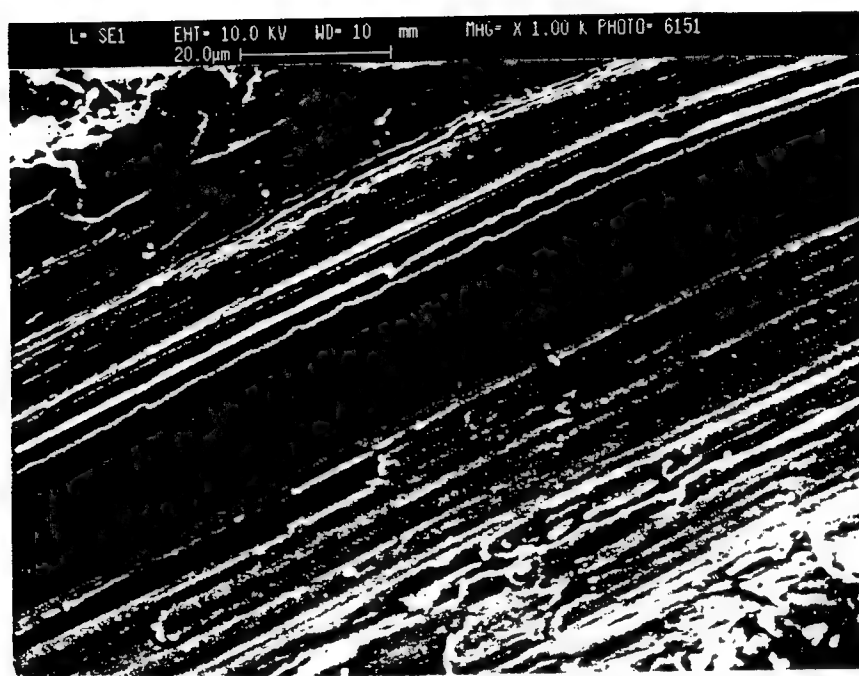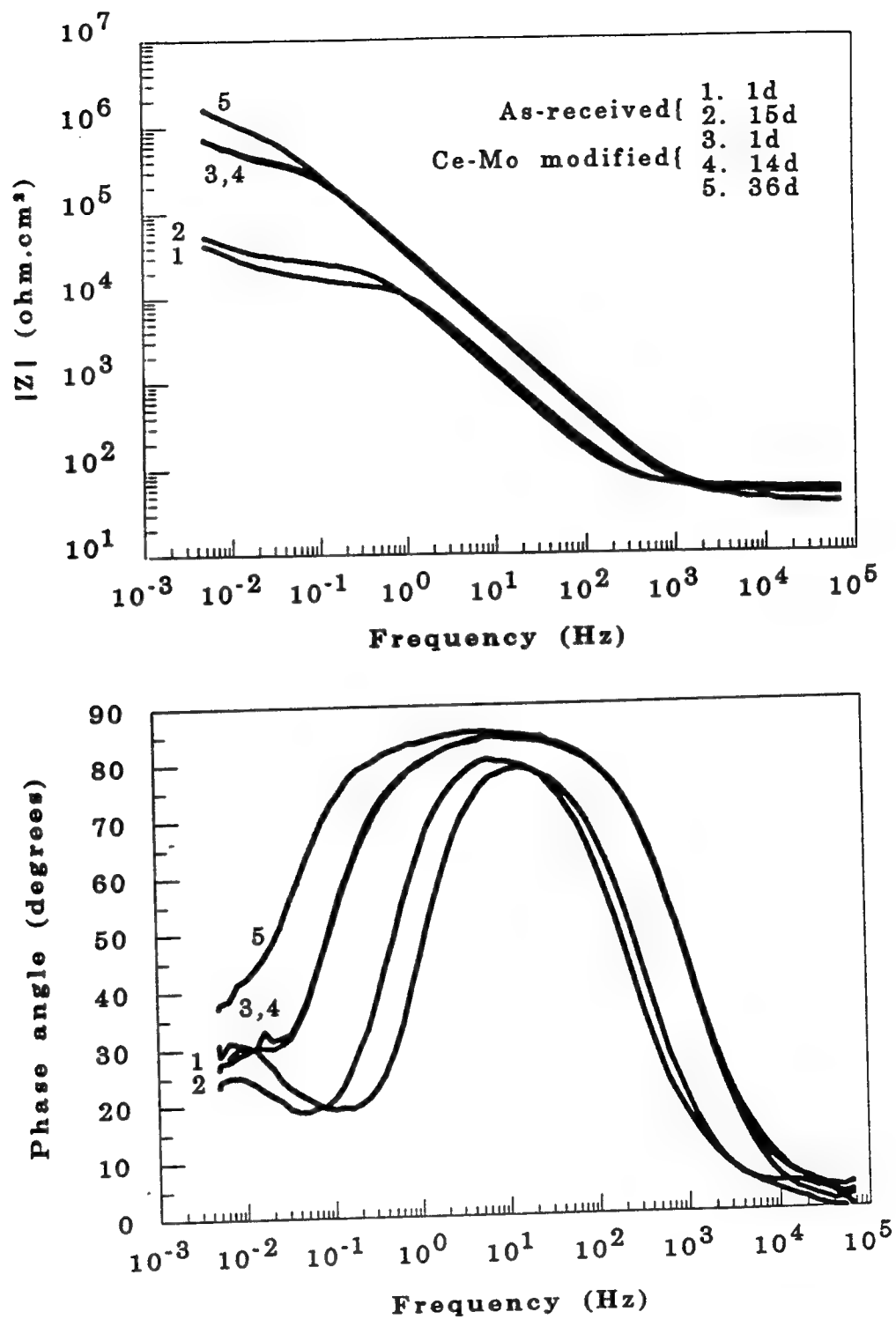
impedance occurred in a very short time. The decrease of impedance at intermediate frequencies and the shift of the phase angle to lower frequencies due to pit propagation were pronounced. For the modified sample, unchanged impedance spectra with time were measured for two weeks. A slight increase of transmission line impedance was observed after 36 days.

Pit initiation was detected after 5 days and pits grew very slowly on the modified surface. At the end of test, five small pits were detected. In Fig. 28 pit propagation represented by the increase of F as a function of exposure time is shown for untreated and modified surfaces. Pits on the untreated sample grew at a fast rate, after 15 days about 1.2% of the exposed area was pitted. However, pit growth for the modified sample was much lower, the estimated value of F was about 0.07% after 36 days exposure.

Salt spray tests according to ASTM B 117 were carried out with both untreated and modified samples at Alcoa. After the 15 days test, severe pitting corrosion was detected for untreated Al 6013, while samples modified by the Ce-Mo process did not show significant corrosion.

3.3   Surface Modified Al 7075 in the As-Received Condition

Surface modification by the Ce-Mo process for pure Al and Al 6061 produced surfaces which are very resistant to localized corrosion. When this process was applied to high-Cu Al alloys such as Al 2024 and Al 7075, less satisfactory results were obtained. Therefore, for surface modification of high-Cu Al alloys, the Ce-Mo process was modified by altering the original treatment procedures. In the modified Ce-Mo process #1 described in Table VI, Al 7075 was used in the as-received condition, deaeration with N_2 before and during polarization in Na_2MoO_4 was eliminated, and the reference electrode of SCE was replaced by mercury sulfate electrode due to avoid Cl^- leaking into the solution during anodic polarization.

For Al 7075 modified in this manner impedance spectra indicated that the modified surface remained passive during the test period of 30 days in NaCl (Fig. 29). R^o_p was nearly constant at about 5×10^5 ohm.cm^2 and C^o_p increased slightly from 7.5 to 9.5 $\mu F/cm^2$ which is typical for a thin film of hydrated aluminum oxide (Fig. 30) [25]. Visually, a few slightly yellow-colored spots of local dissolution were observed after 4 days which grew very slowly.

Examination by SEM after exposure to NaCl for 30 days showed that the morphology of the observed spots was quite different from pitting corrosion phenomena usually occurring on Al alloys (Fig. 31). A circular area, typically about 60 μm in diameter, with cracks in the oxide layer was observed (Fig. 31 a). Some areas of very small dimensions with localized attack can be seen at the periphery of these circular features. Fig. 31 b shows more detailed information from the center of the spot in Fig. 31 a. Cracks radiating from the center ended at a short distance. The chemical composition was determined by EDS for the surface in Fig. 30 and for a portion of the sample which had not been exposed. The results are given in Fig. 32 a for the unexposed surface and in Fig. 32 b for the surface area shown in Fig. 31. In both cases, Ce and Mo were detected in the surface layer, however, increased levels of Ce and Mo were determined in the surface area where the cracked spots were detected.

Elemental mapping was employed to obtain concentration profiles of Ce and Mo in the modified surface layers. Results for the area shown in Fig. 31 are presented in Fig. 33. It is interesting that the chemical composition of the surface layer is different in an inner circle and an
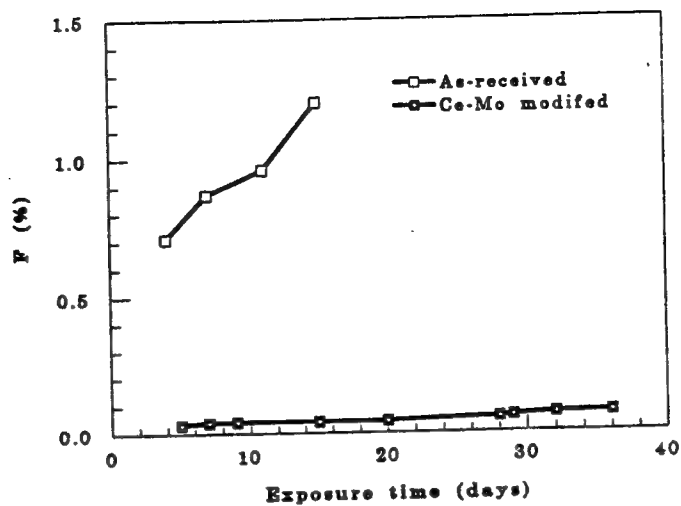
Fig. 28. Time dependence of area fraction F for Al 6013 (as-received vs. surface modified)

Fig. 29. Impedance spectra for Al 7075/as-received/Ce-Mo process #1 as a function of exposure time to 0.5 M NaCl
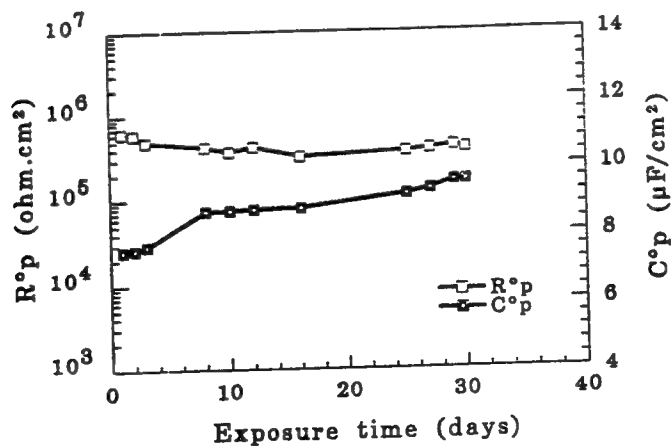
Fig. 30. R^o_p and C^o_p for Al 7075/as-received/Ce-Mo process #1 as function of exposure time

a)

b)
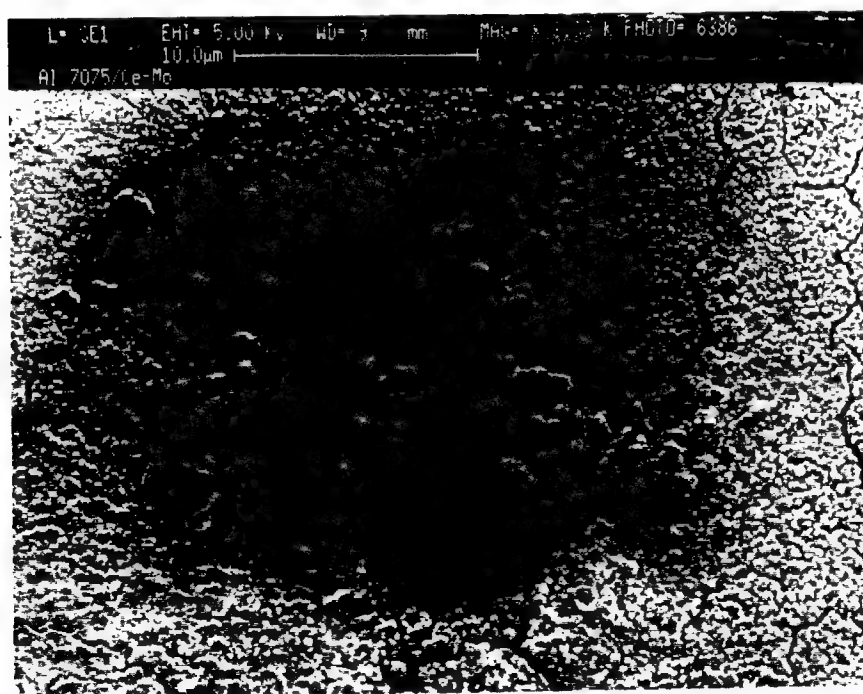
Fig. 31. Surface morphology for Al 7075/as-received/Ce-Mo process #1
after exposure to 0.5 M NaCl for 30 days
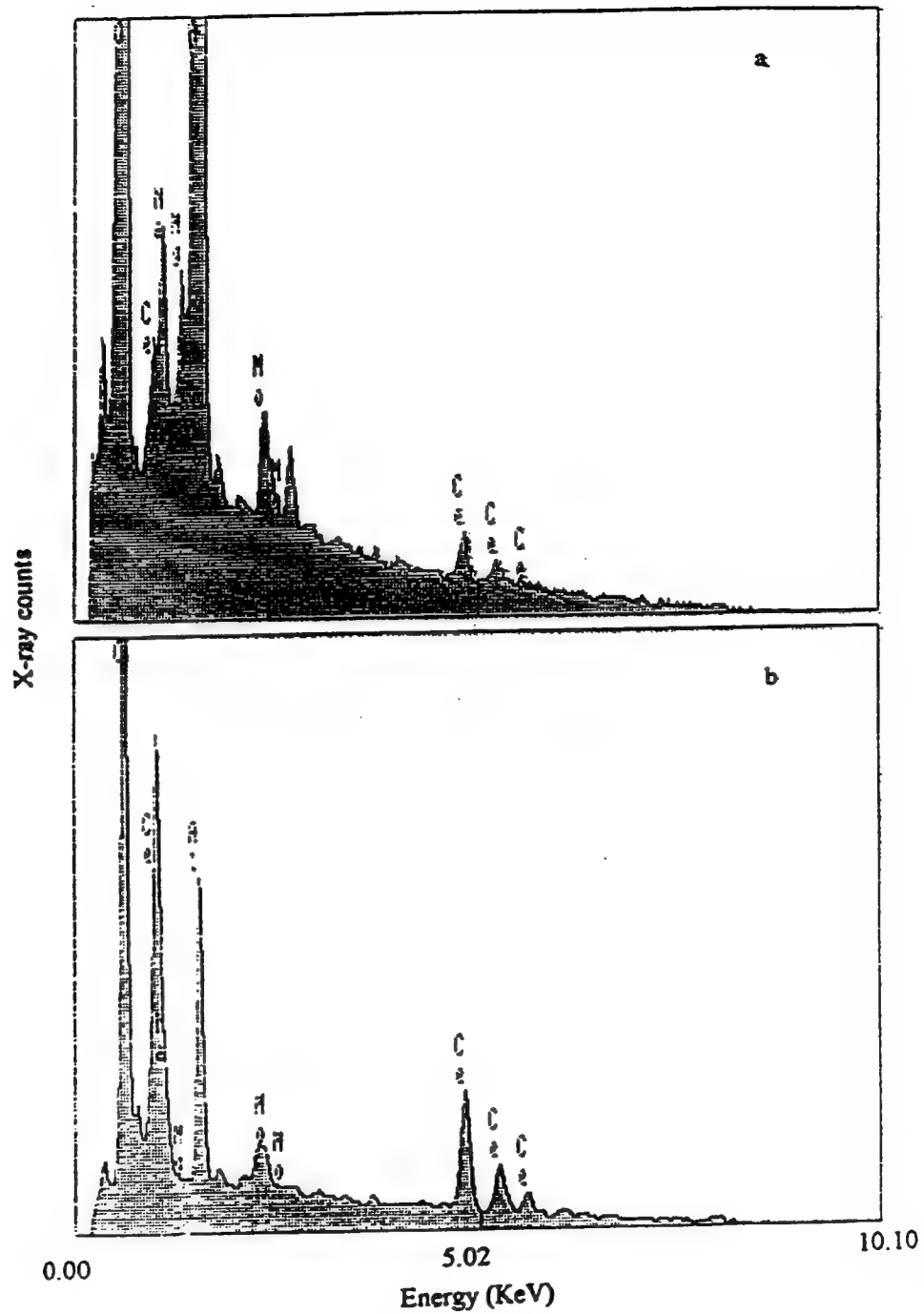
Fig. 32. Chemical composition of surface layers on Al 7075/as-received/Ce-Mo process #1; a) unexposed surface, b) corrosion spot after exposure to 0.5 M NaCl for 30 days
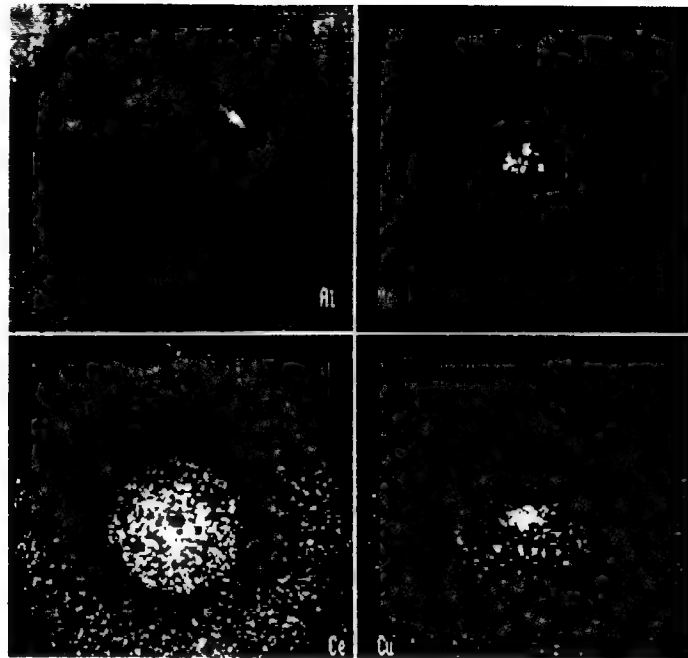
Fig. 33. Elemental mapping for Al 7075/as-received/Ce-Mo process #1 (sample in Fig. 31)

outer ring. Ce is concentrated in the inner circle and Mo resides in the center where Cu intermetallic compounds are located. Very little Al was detected in the inner circle. These results can be explained by assuming that during surface modification by the Ce-Mo process, Cu containing intermetallic compounds served as cathodes creating an alkaline environment in their vicinity, thereby accelerating local dissolution of Al and leading to formation of Ce oxide and/or Ce hydroxide around these compounds [44,45]. A similar pattern of Ce precipitates on Al 2024 immersed in $CeCl_3$ has also been observed [46]. Incorporation of Mo into the surface film is considered to be the result of interaction between molybdate and aluminum oxide during anodic polarization in Na_2MoO_4 [22,47,48]. The observed cracks occurred during exposure to NaCl because they were not observed after treatment in the Ce-Mo process.

In order to further evaluate the mechanism of surface modification and the resulting resistance to localized corrosion, anodic polarization curves were obtained in 0.5 M NaCl for Al 7075/as-received and Al 7075/as-received modified by the modified Ce-Mo process #1 (Table VI). The polarization curve for modified Al 7075 showed a passive region of approximately 200 mV. The passive current density ranged from 0.1 - 0.5 $\mu A/cm^2$ (Fig. 34). During continued anodic polarization, sudden jumps of the current were observed accompanied by formation of single pits. The polarization curve is very different from that for Al 7075/as-received, for which E_{pit} and E_{corr} coincided (Fig. 34) and for which the current dramatically increased during increased anodic polarization as pits nucleated and grew. Obviously, the increased pitting resistance for the modified surface was due to the increase of E_{pit} at constant E_{corr}. This effect might be due to changes in surface chemistry of the modified surface layers, on which cathodes, which would lead to pit initiation for the untreated surface, have been passivated during the surface modification process by the formation of Ce oxide/hydroxides and incorporation of Mo species.

3.4   Surface Modification of Al 7075 and Al 2024 with Cu Removal Pretreatment

Complete elimination of localized corrosion for Al 7075 was achieved by applying a Cu removal pretreatment step before the modified Ce-Mo process #1 (Table VI). Significant improvement was also obtained for Al 2024. The electrochemical Cu removal process (Table IV) was utilized to obtain surface layers with reduced Cu content. The surface morphology of Al 7075 after electrochemical Cu removal shows some cavities from which Cu containing compounds had been removed, the remaining surface was undamaged (Fig. 35). Following the Cu removal step, the modified Ce-Mo process #1 (Table VI) was applied to Al 7075 (Al 7075/Cu removal/Ce-Mo process) and Al 2024 (Al 2024/Cu removal/Ce-Mo process).

3.4.1   Al 7075/Cu removal/Ce-Mo process

For Al 7075, very corrosion resistant surfaces were produced in the modified Ce-Mo process #1. The evaluation of the corrosion resistance in NaCl showed that the resulting surfaces were entirely passive. In Fig. 36 impedance spectra collected at E_{corr} are shown as a function of exposure time. For a test period of 30 days, no measurable corrosion was indicated and the impedance remained capacitive. R^o_p and C^o_p did not change significantly with exposure time (Fig. 37). High values of R^o_p (about 10^6 $ohm.cm^2$) and constant C^o_p suggest that the modified surface was very resistant to pitting in aggressive environments such as 0.5 M NaCl.

Fig. 34. Anodic polarization curves in 0.5 M NaCl for Al 7075
(as-received vs. surface modified)

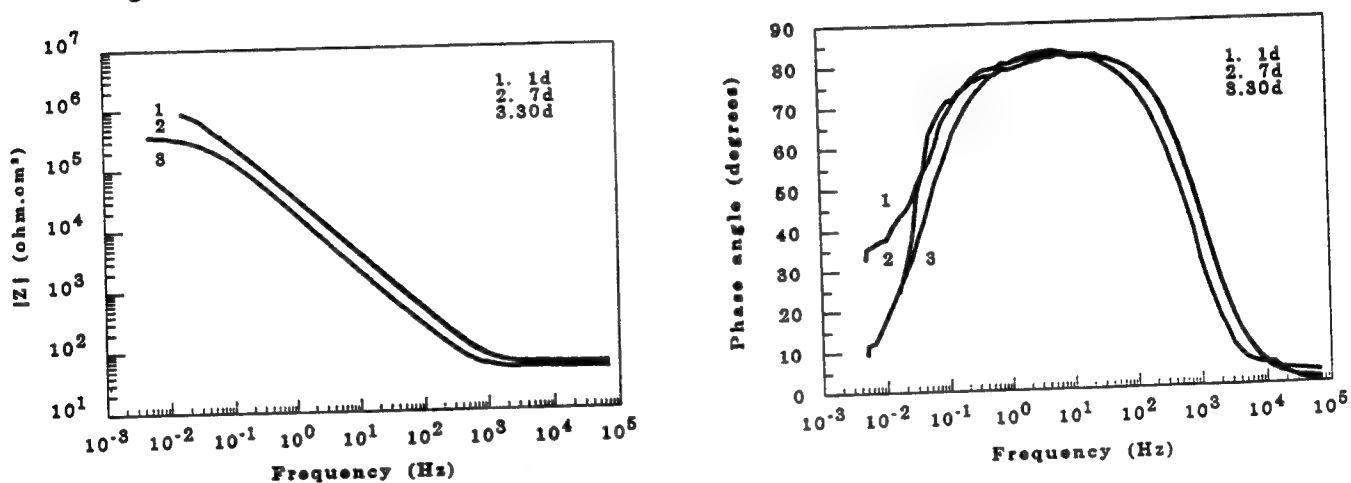Fig. 35.   Surface morphology of Al 7075 after Cu removal

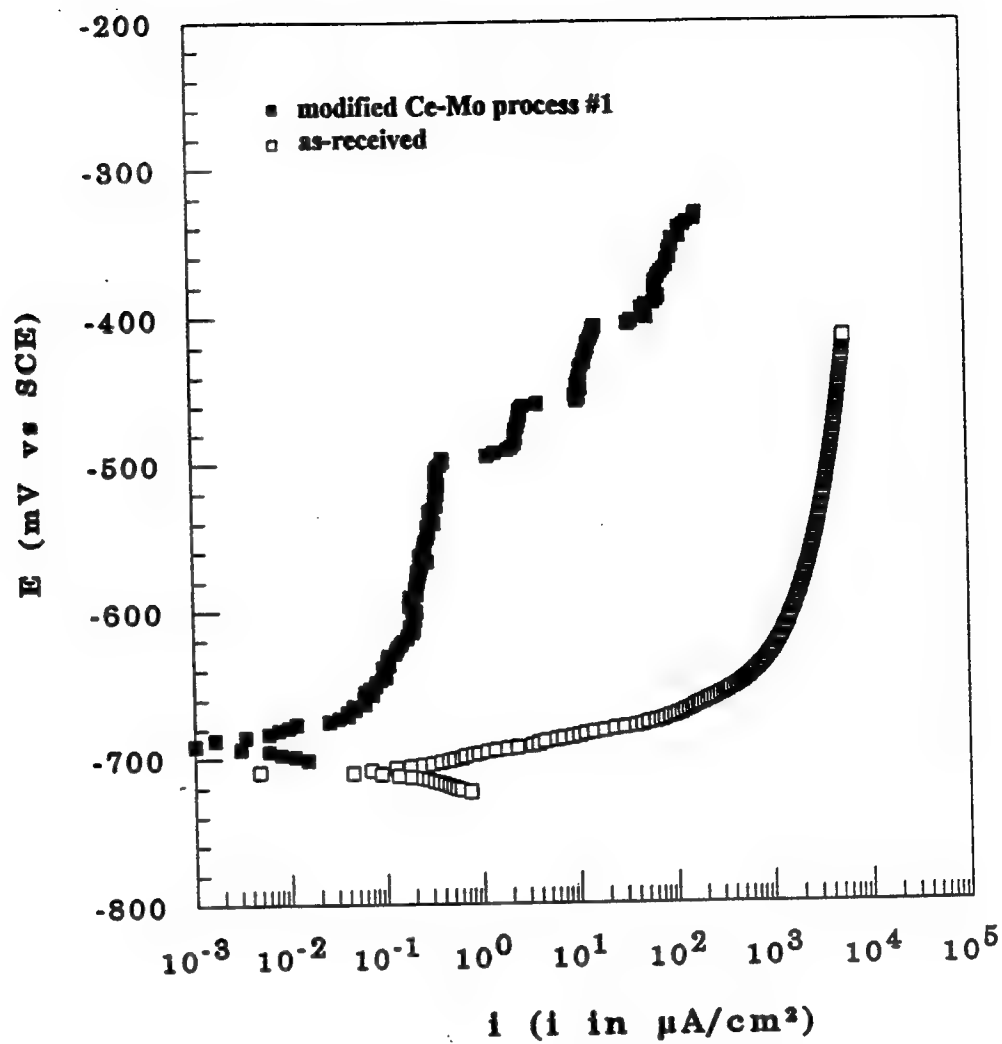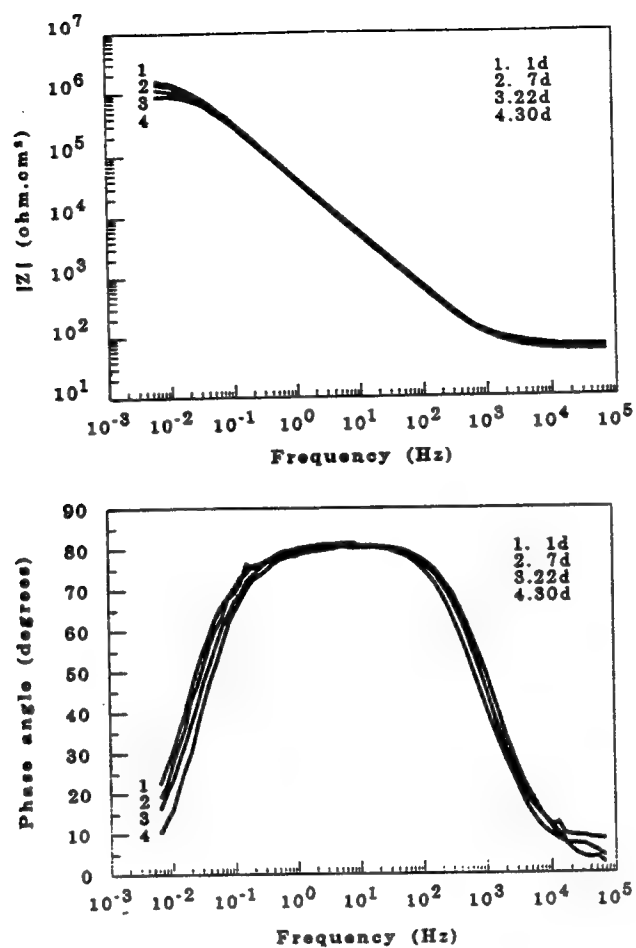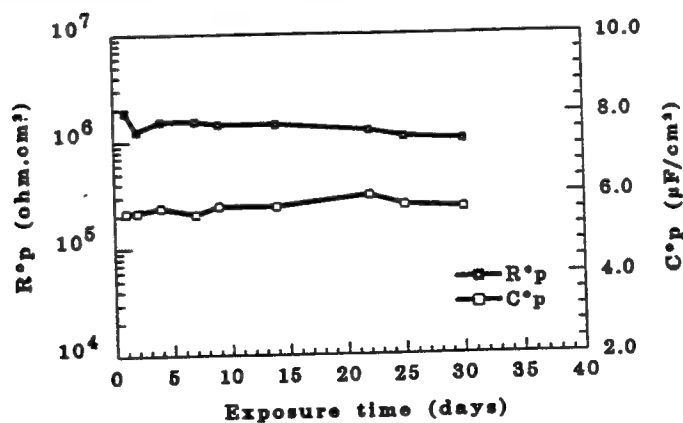Fig. 36. Impedance spectra for Al 7075/Cu removal/Ce-Mo process #1 as a function of exposure time to 0.5 M NaCl

Fig. 37. R^o_p and C^o_p for Al 7075/Cu removal/Ce-Mo process #1 as function of exposure time

3.4.2 Al 2024/Cu removal/Ce-Mo process

For Al 2024 treated in the modified Ce-Mo process #1, no considerable changes of the surface properties due to corrosion were indicated by EIS (Fig. 38). It should be mentioned that a few pits initiated between 4 and 7 days. After one week, no additional pit initiation was observed by visual inspection. At the end of the test, 13 small pits with $F = 6.5 \times 10^{-4}$ were detected. The total pitted area $A_{pit} = 0.026$ cm^2 was much smaller than that for the sample with Cu removal only for which F was determined as 8.10^{-2} after exposure to 0.5 M NaCl for 7 days, and pit initiation occurred after less than 2 hours as determined by visual inspection.

3.5   Surface Modification of Al 2024 in the Modified Ce-Mo Process #2

Further optimization of the modified Ce-Mo process for Al 2024 consisted of immersion in hot $(CH_3CO_2)_3Ce$, polarization in Na_2MoO_4 and immersion in hot $Ce(NO_3)_3$ (the modified Ce-Mo process #2, Table VII). Very corrosion resistant surfaces were obtained for surface modified Al 2024.
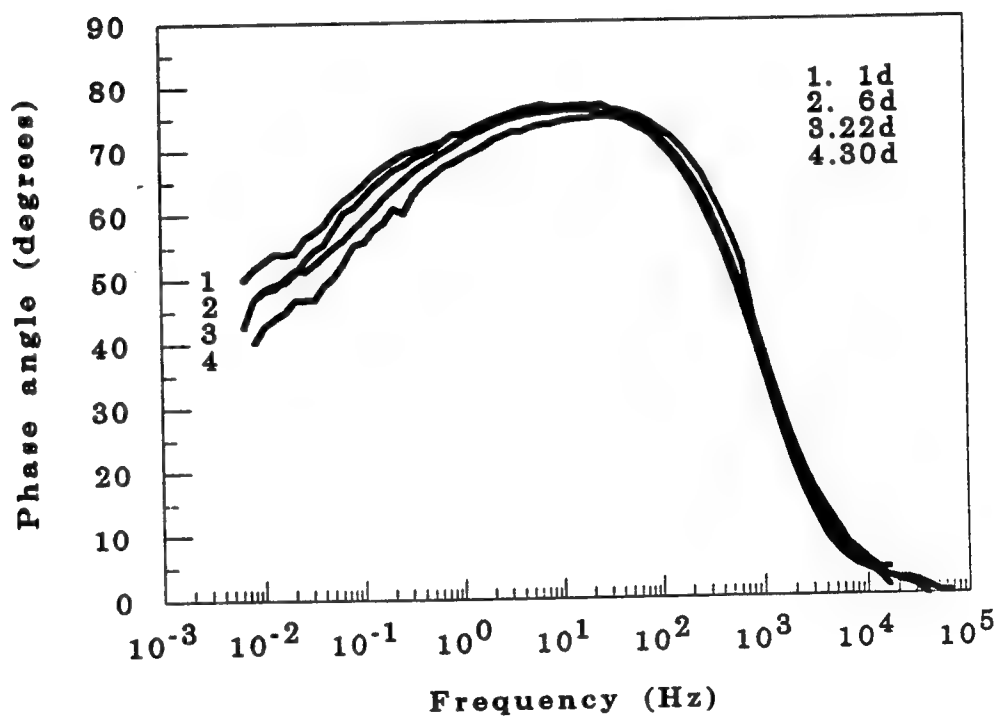
3.5.1 Impedance Spectra

For surface modified Al 2024, impedance spectra did not show signs of localized corrosion and no significant changes between the first and the last day of exposure occurred (Fig. 39). R^o_p was about 4×10^6 ohm.cm^2 and C^o_p increased slightly from 7 to 9 µF/cm^2 (Fig. 40). Visually, at the end of the test, one very small pit with 0.6 mm in diameter was observed for an exposed area of 20 cm^2, which is below the detection limit of EIS [34]. Therefore, the spectra in Fig. 39 did not show the typical features of localized corrosion characterized by a transmission line impedance at lower frequencies (Fig. 4 - 6).

3.5.2 Polarization Curves

Anodic polarization curves for as-received and surface modified Al 2024 are shown in Fig. 41. E_{pit} increased at constant E_{corr}, resulting in a passive region of about 80 mV and i_p was less than 3 µA/cm^2. This anodic polarization behavior is similar to the results obtained for Al 6061/Ce-Mo process (Fig. 12) and for modified Al 7075/as-received (Fig. 34). At E_{pit} pits initiated as indicated by local gas evolution. With increasing polarization new pits were generated corresponding to the sharp increase of the current at -475 mV. In Fig. 41 the polarization curve for untreated Al 2024 is also shown, for which pits develop at E_{corr} and grow upon anodic polarization.

3.5.3 Electrochemical Noise Measurements

In addition to monitoring by EIS, electrochemical potential and current noises data were recorded simultaneously for as-received and modified Al 2024 after 1, 12 and 24 hour exposure to 0.5 M NaCl. Fig. 42 shows experimental potential and current noise data after exposure for 1 hour and 24 hours. For Al 2024/as-received, rapid potential and current fluctuations of high amplitude were observed at the start of exposure. With increasing time, E_{corr} shifted to -700 mV, and both potential and current fluctuations diminished. For Al 2024 treated in the modified Ce-Mo process #2, current fluctuations were very low, while the potential fluctuated slowly on a large scale and stabilized at -565 mV at the end of the measurement (Fig. 42 b). Fig. 43 shows the

Top plot

10^7
10^6
10^5
10^4
10^3
10^2
10^1

$|Z|$ (ohm.cm²)

1
2
3
4

1. 1d
2. 9d
3.21d
4.30d

10^{-3} 10^{-2} 10^{-1} 10^0 10^1 10^2 10^3 10^4 10^5

Frequency (Hz)

Bottom plot

90
80
70
60
50
40
30
20
10
0

Phase angle (degrees)

1
2
3
4

1. 1d
2. 6d
3.22d
4.30d

10^{-3} 10^{-2} 10^{-1} 10^0 10^1 10^2 10^3 10^4 10^5

Frequency (Hz)
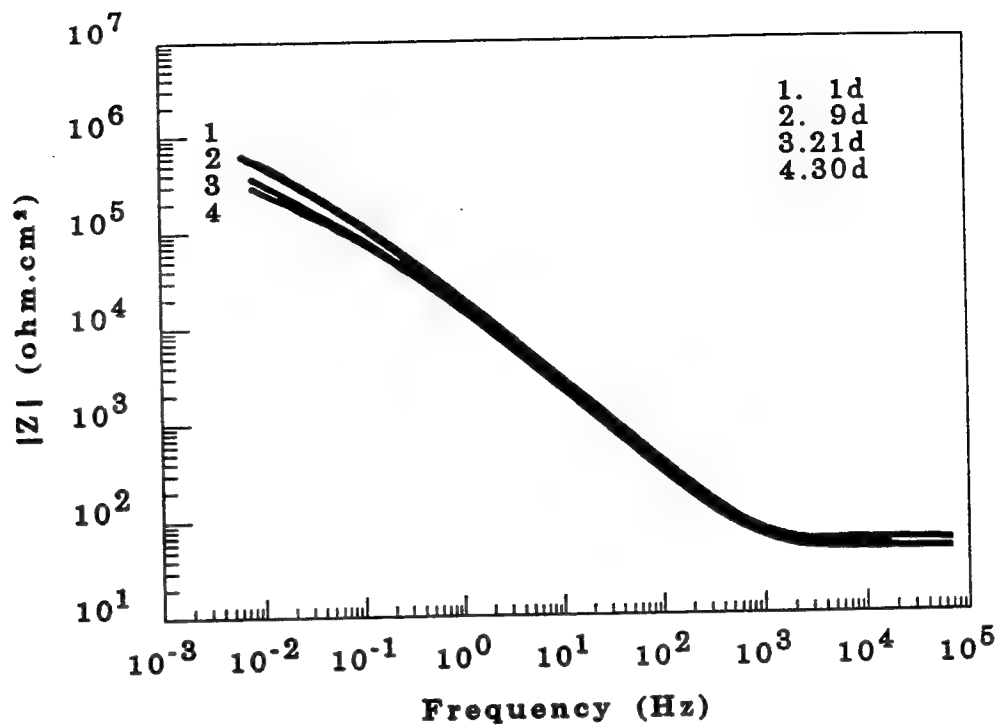
38. Impedance spectra for Al 2024/Cu removal/Ce-Mo process #1 as a function of exposure time to 0.5 M NaCl
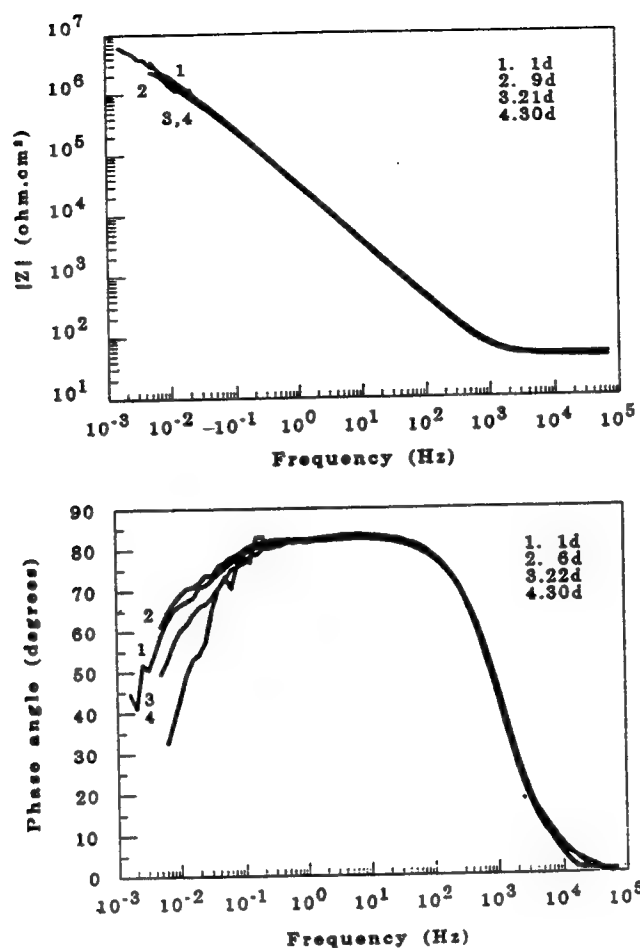
Fig. 39. Impedance spectra for Al 2024/Cu removal/Ce-Mo process #2 as a function of exposure time to 0.5 M NaCl
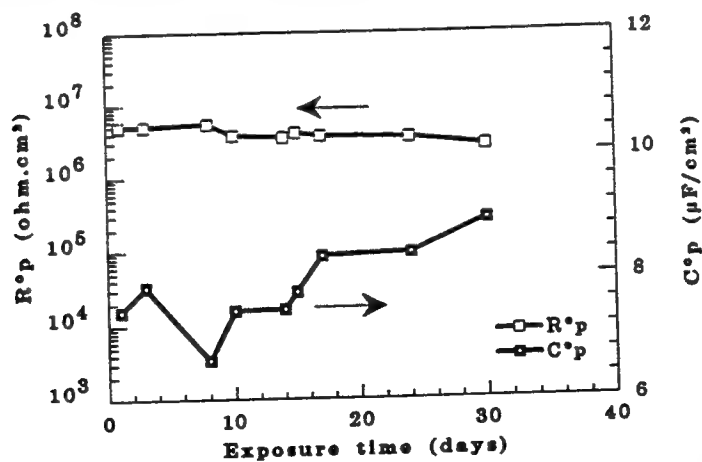
Fig. 40. R^o_p and C^o_p for Al 2024/Cu removal/Ce-Mo process #2 as function of exposure time
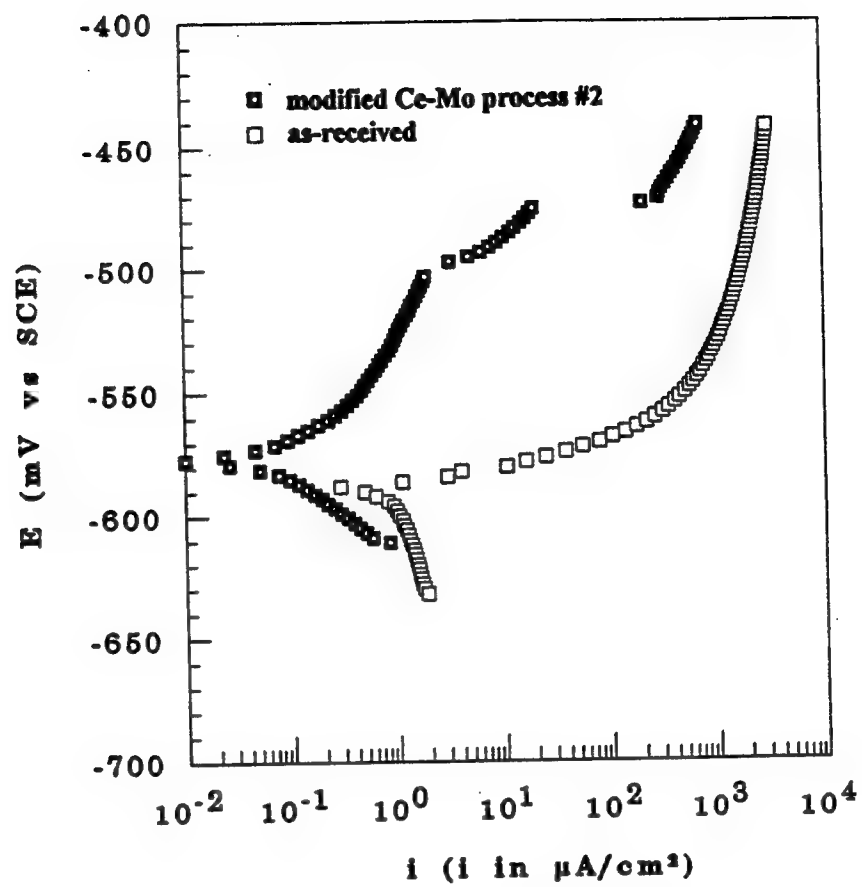
Fig. 41. Anodic polarization curves in 0.5 M NaCl for Al 2024/as-received and Al 2024/Cu removal/Ce-Mo process #2
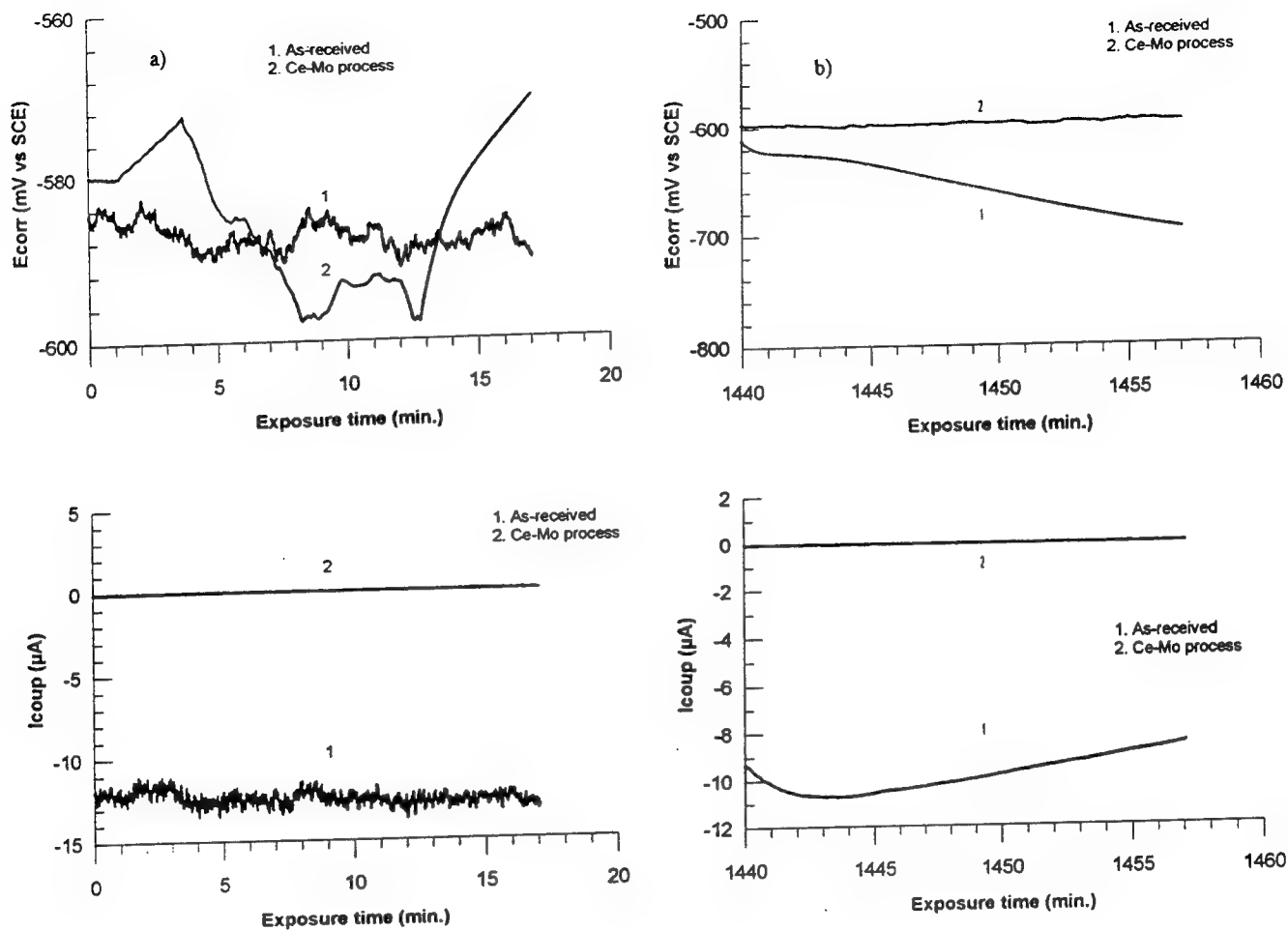
Fig. 42. Potential and current noise data recorded for Al 2024/as-received and
Al 2024/Cu removal/Ce-Mo process #2; a) after 1 hour, b) after 24 hours
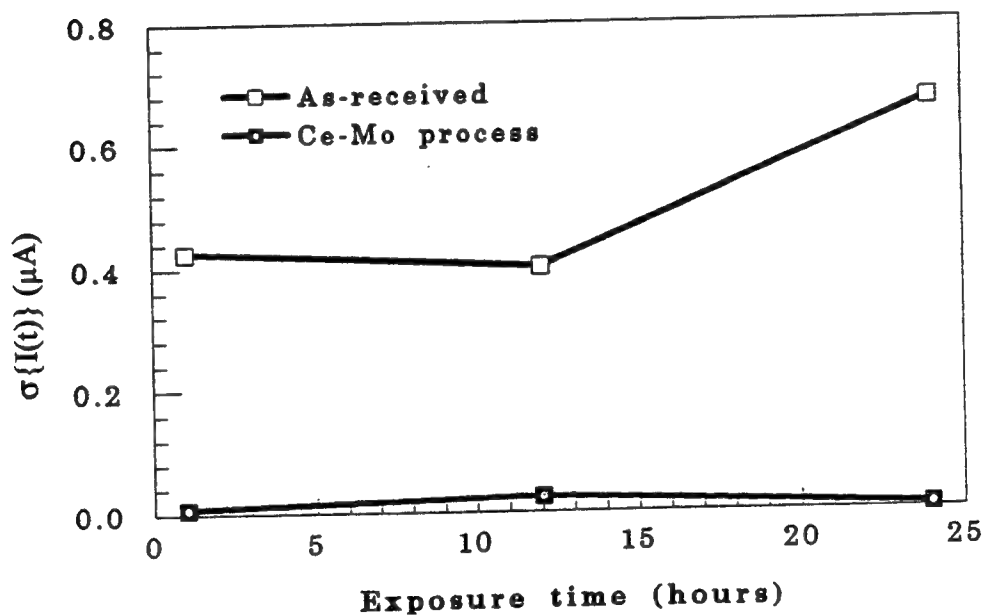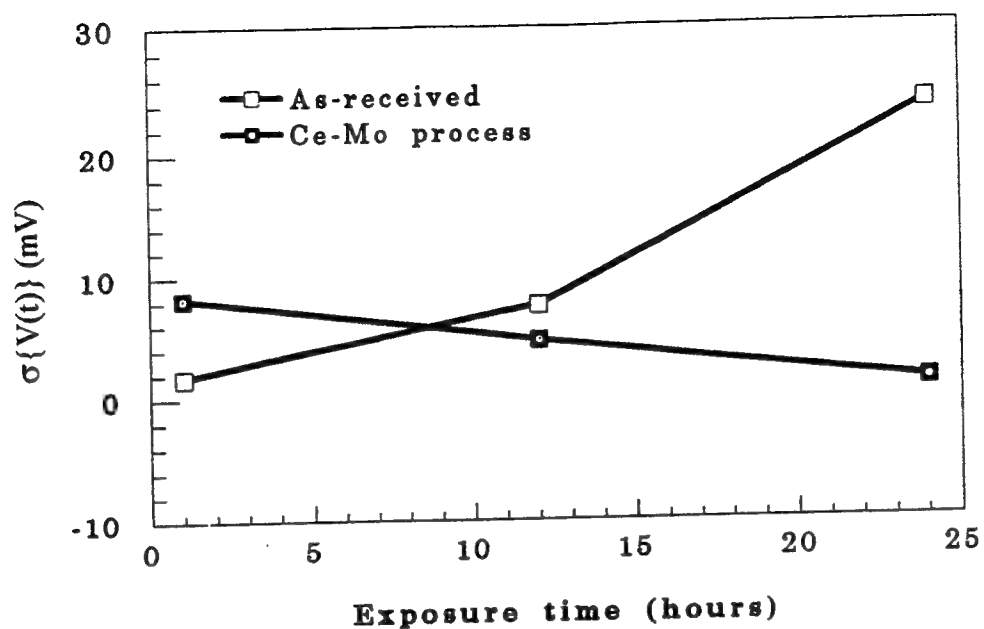
Fig. 43. Potential and current standard deviations for Al 2024/as-received and Al 2024/Cu removal/Ce-Mo process #2 as function of exposure time

standard deviation values of potential ($\sigma\{V(t)\}$) and current ($\sigma\{I(t)\}$) during 24 hours exposure. Large values of $\sigma\{I(t)\}$ and an increase of $\sigma\{V(t)\}$ with time were observed for Al 2024/as-received. For Al 2024/Ce-Mo process, $\sigma\{I(t)\}$ was less than 0.02 μA, and $\sigma\{V(t)\}$ decreased from 8 mV to 3 mV within 24 hours.

In Fig. 44a, the noise resistance R_n, which is derived from the data in Fig. 43 according to Eq. 2-1, is plotted as a function of time. R_n values ranging from 2×10^6 to 6×10^6 ohm.cm^2 were obtained for the surface modified Al 2024, while the values of R_n for Al 2024/as-received were much lower. Fig. 44b shows the time dependence of R^o_{sn} (Eq. 2-4) for as-received and modified Al 2024 during exposure to NaCl. Very similar values and time dependence of R^o_{sn} were obtained. More detailed information concerning the corrosion behavior of these two different surfaces can be seen from plots of R_{sn} vs. frequency obtained by spectral analysis according to Eq. 2-3. R_{sn} spectra for Al 2024/as-received showed increased magnitude with increasing time (Fig. 45 a) and the values of R_{sn} were much lower, while constant R_{sn} spectra with high value were determined for Al 2024/Ce-Mo process sample (Fig. 45 b).

4. DISCUSSION

4.1 Localized Corrosion of Aluminum Alloys

Localized corrosion in the form of pitting was recognized in the early 1900's as aluminum corroded in salt solutions with metallic impurities enhancing corrosion rates [49]. Over the last 80 years, many investigations have been conducted dealing with pit initiation, propagation and mechanisms of pitting corrosion [50-54]. Attempts have also been made to evaluate the pitting susceptibility of different Al alloys using electrochemical parameter such as E_{pit} [55-57].

Often the pitting potential E_{pit} is used to estimate the susceptibility of different materials to pitting in a certain environment. However, for Al alloys exposed to aerated media containing halides the use of E_{pit} is unsatisfactory for the characterization of pitting susceptibility. Experimental findings have demonstrated that for Al alloys exposed to NaCl solutions, E_{pit} and E_{corr} are almost identical (Table IX) and these alloys pitted. Moreover, the total extent of pitting was much higher for Cu-bearing alloys such as Al 2024, which has a noble pitting potential (-588 mV) than other Al alloys such as Al 6061, which has a more negative pitting potential (-725 mV).

Generally, E_{pit} depends on the nature and the concentration of pit-inducing ions. Experimental and theoretical evidences indicate that E_{pit} decreases with increasing concentration of Cl$^-$ [52]. Augustynski [58] showed that the surface concentration of Cl$^-$ increased from 3 % at E_{corr} to 12-13% at E_{pit}. Although there is less discussion about the relationship between E_{pit} and the concentration of Cl$^-$ absorbed on the surface, E_{pit} may be thought of as a parameter indicative of surface adsorption of pit-promoting ions, at which the concentration of adsorbed pit-promoting ions reaches a critical value. As will be discussed below, the increase of E_{pit} at constant E_{corr} for modified surfaces of Al alloys is considered to be due to inhibition of Cl$^-$ adsorption on oxide layers containing Ce and Mo, thereby increasing pitting resistance.

EIS was found to be a very powerful tool to characterize pit initiation and pit propagation processes for Al alloys exposed to NaCl. Pit initiation can be detected by characteristic changes of impedance spectra. Mansfeld et al. [42,59,60] utilized EIS to study pitting corrosion of Al 7075-
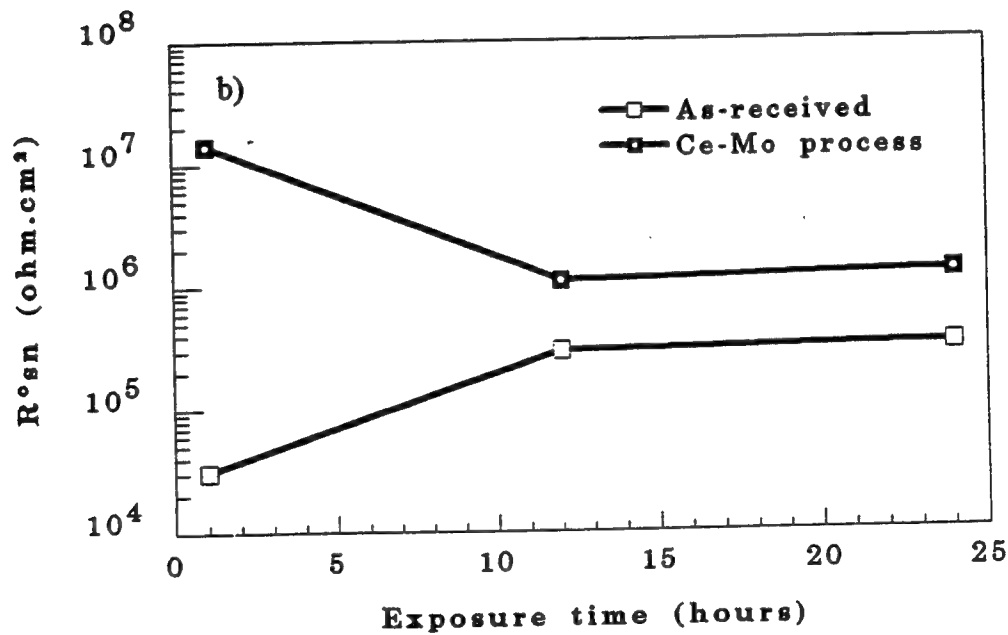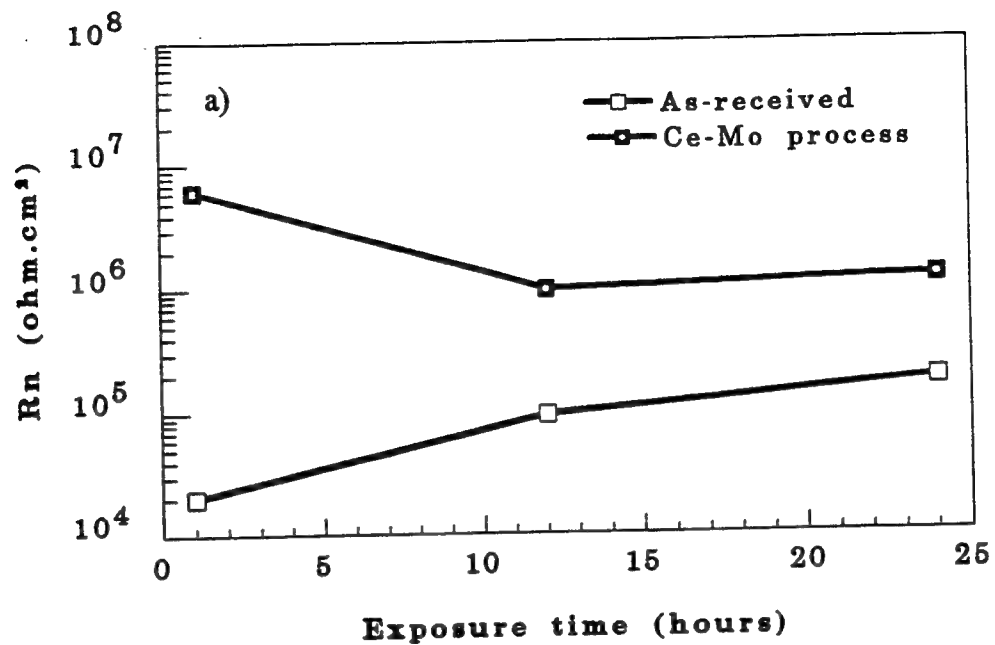
Fig. 44. Time dependence of R_n and R^o_{sn} for Al 2024/as-received and Al 2024/Cu removal/Ce-Mo process #2
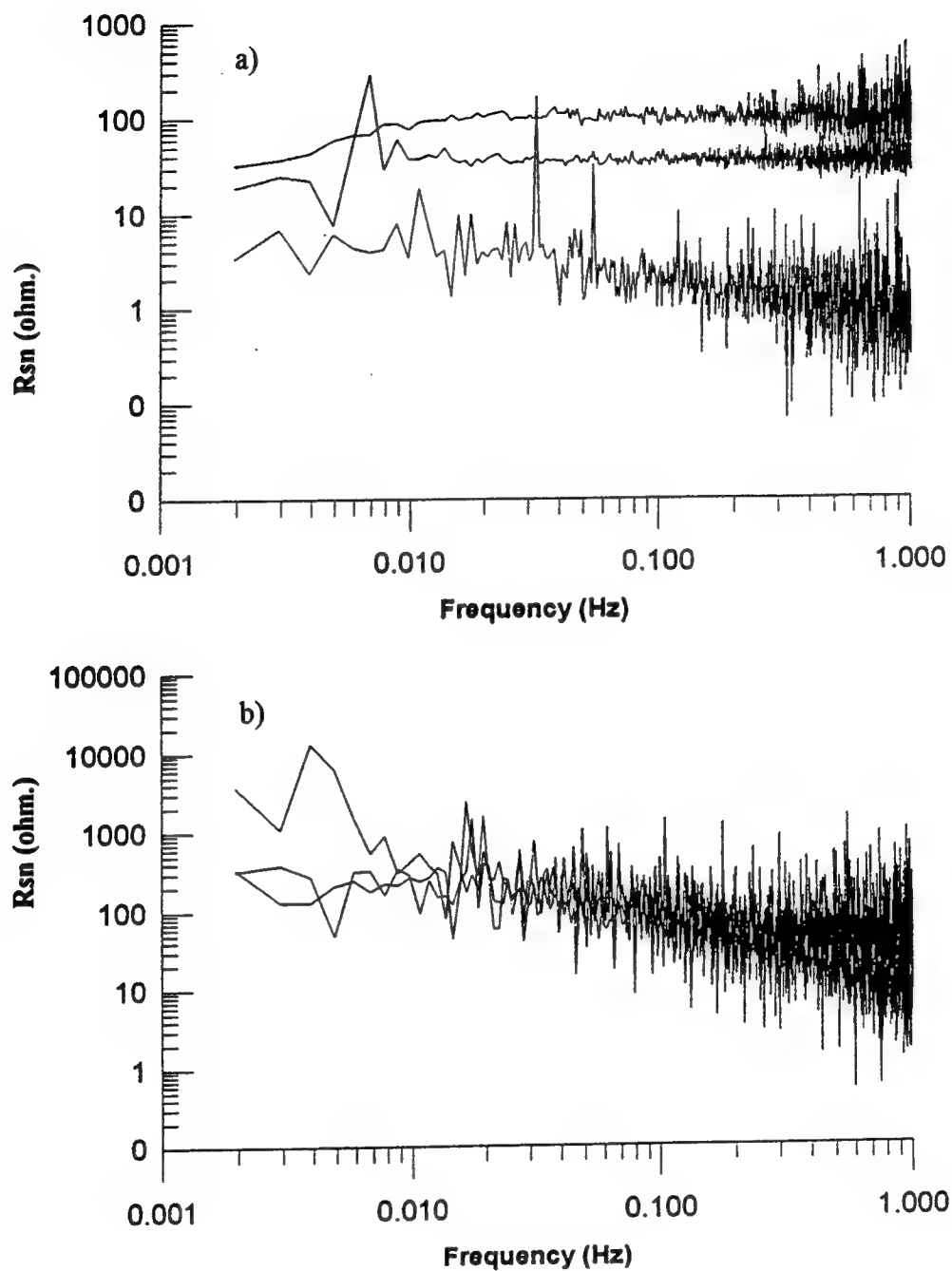
Fig. 45. Frequency dependence of R_{sn} for Al 2024/as-received (a)
and Al 2024/Cu removal/Ce-Mo process #2 (b)

T6 and Al 7075-T73 in NaCl, which were untreated or passivated in $CeCl_3$. The experimental results indicated that when pits initiated, the EIS spectra changed from capacitive impedance to transmission line impedance at lower frequencies, and the impedance decreased in the intermediate frequency range. Systematic studies for Al 2024, Al 6061, and Al 7075 exposed to 0.5 M NaCl illustrate that once pitting corrosion occurs, the impedance spectrum is characterized by the occurrence of transmission line impedance and a second time constant in the phase angle plot at lower frequencies, which is a sensitive indicator of localized corrosion (Fig. 4 - 6). With increasing exposure time, the pronounced changes of the phase angle, together with the decrease of the impedance at the intermediate frequency region, allow to detect the presence of active pits and to monitor the pit propagation process.

Pit growth rates for Al alloys were determined based on the EIS data collected at E_{corr} as a function of time. Quantitative analysis of the time dependence of R^o_{pit} allowed derivation of pit growth rates expressed by $1/R^o_{pit}$ as a function of time according to Eq. [3-1] and [3-2]. For untreated Al alloys experimental value of b ranged from -1.38 for Al 7075/as-received to -0.86 for Al 2024/deoxidized [34]. Assuming b = -1, pit growth rates were found to decrease with increasing exposure time and the radii of hemispherical pits were found to increase logarithmically with increasing exposure time. The experimental approach used in the present study was different from previous evaluations of pit growth laws [61 - 64] since the experimental data were collected at E_{corr} instead of $E > E_{pit}$. For surface modified Al alloys pits did not initiate within the minimum test period of 30 days.

4.2   The Ce-Mo Process

Molybdate is known to reduce the susceptibility of stainless steels and Al alloys to pitting. The research group at Martin Marietta has evaluated methods of corrosion protection of Al which include production of Al-Mo alloys by RF sputter deposition of Al onto single crystal Si wafers [25]. The corrosion resistance of the resulting surface alloy layers was examined by potentiodynamic polarization curves. E_{pit} was found to increase from - 700 mV for untreated surfaces to -100 mV for alloy surfaces with Mo concentrations between 5% and 10%. Shaw et al. [29] reported results obtained with an electrochemical process in which Mo claimed to be in the +4 and +6 valence states was incorporated into the oxide film on sputter-deposited Al foil on Si single crystal. This anodic polarization procedure in 1000 ppm Na_2MoO_4 led to a significant shift E_{pit} in the noble direction for treated surface immersed in NaCl. Because of this positive shift of E_{pit} at constant E_{corr}, the authors concluded that the modified passive film was resistant to pitting. Similar surface films containing Mo, called molybdate conversion coatings, were also obtained by immersing Al 7075 in deaerated 0.01 M Na_2MoO_4 [18]. A trend of increasing E_{pit} was observed for these molybdate conversion coated surfaces in deaerated 0.01 M NaCl. Based on these results, molybdate conversion coatings were considered to provide corrosion protection for Al alloys. Molybdate conversion coatings have been produced on several Al alloys, however none of these methods provided corrosion protection comparable to that provided by chromate conversion coatings. In the present study [34], application of the methods described by Shaw et al. [29] and Hinton et al. [18] for Al 6061 showed that upon exposure to 0.5 M NaCl, both pitting and uniform corrosion occurred after a short time to the same extent for treated and for untreated surfaces.

The Ce-Mo processes were developed as new approaches for corrosion protection of Al alloys without use of toxic chemicals and applied to pure Al, Al 6061, Al 6013, Al 2024 and Al 7075. The problems with the use of molybdate conversion coatings [18] and chemical passivation in REM salts [44,65-69] were not encountered in the applications of these processes. From the previous studies it is known that treating Al alloys in Ce salt solutions induces formation of mixed

Al-Ce oxide layers. These Al-Ce oxides are very stable in NaCl due to their low solubility, thereby increasing the corrosion resistance of Al alloys. In addition, Mo has been reported to be incorporated into the oxide on Al alloys by anodic polarization in molybdate solutions, leading to increased E_{pit} [18,25,29]. With the objective of incorporating Ce and Mo into aluminum oxide layers by a combination of chemical passivation and electrochemical techniques, the Ce-Mo process initially consisted of treatment in Ce salt solutions, followed by anodic polarization in Na_2MoO_4 (Table VII). Applying this process to Al and its alloys produced very corrosion resistant surfaces with exceptional resistance to pitting.

4.2.1. Corrosion Behavior of Surface Modified Al 6061

Surfaces of Al alloys modified by the Ce-Mo process were very corrosion resistant in chloride-containing environments. For Al 6061 treated in the Ce-Mo process, impedance spectra remained capacitive and no evidence of localized corrosion was indicated by EIS and by visual inspection for 30 days. Uniform corrosion rates were determined to be about 0.05 μm/year for $R^o_p = 10^7$ ohm.cm^2. This value is lower than that obtained for SS 304 exposed to the same environment, for which corrosion rate was determined to be 0.19 μm/year based on $R^o_p = 7 \times 10^5$ ohm.cm^2 [70]. The outstanding properties of modified surfaces are reflected in the polarization behavior in 0.5 M NaCl. As shown in Fig. 12 and 13, very interesting polarization curves were recorded. E_{pit} increased to -325 mV, which is more than 400 mV positive to E_{corr}. This separation of E_{corr} and E_{pit} is indicative of pit resistant surfaces. In the passive region, i_p was as low as 3 μA/cm^2. When E_{pit} was reached, a few pits initiated, while the remainder of the surface was unattacked. To our knowledge, polarization curves such as those shown in Fig. 12 and 13 have not been reported before for Al alloys in NaCl.

Another illustration of corrosion resistant surfaces are the results obtained for modified Al 6013 exposed to NaCl, on which a few pits developed between 3 and 4 days and propagated with extremely low rates. Most pits were found to be located at sites where existing surface defects apparently had not been passivated during surface modification. For 36 day exposure, only a small pitted area fraction (F = 0.0007) was determined.

It is clear that the modified surface layers formed in the Ce-Mo process are quite different from those formed by immersion in Ce salt solution, for which E_{corr} shifted in the negative direction due to the suppression of the rate of oxygen reduction, while E_{pit} remained unchanged [34]. The exceptional pitting resistance produced by the Ce-Mo process is attributed to the increased E_{pit} at constant E_{corr}. Since E_{pit} shifted far above E_{corr}, the attack of Cl$^-$ at E_{corr} was diminished. Although it is difficult to explain how E_{pit} is related to adsorption of Cl$^-$ at the surface/electrolyte interface, experimental results have illustrated that E_{pit} decreases with increasing Cl$^-$ concentration in the bulk solution probably due to increased concentration of absorbed Cl$^-$ on the interface [52,58]. This evidence clearly points out that pit initiation strongly depends on the concentration of adsorbed Cl$^-$ on the Al surface. For surfaces modified by the Ce-Mo process due to the presence of Mo in the surface layers which was indicated by EDS (Fig. 20), the amount of adsorbed Cl$^-$ decreases at a given potential. With increasing polarization to E_{pit}, adsorption of Cl$^-$ reaches a critical concentration at which pits initiate, while at potentials below E_{pit} adsorption of Cl$^-$ is not high enough to induce pitting. Addition of small amounts of Mo to Al has been known to increase E_{pit} remarkably [71].

For modified pure Al exposed to 0.5 M NaCl, passive features were indicated by unchanged impedance spectra during exposure (Fig. 22). No pits were detected at the end of the test by microscopic observation. For modified Al with a mechanical scratch corrosion reactions did not occur on the bare aluminum in the scratch during 25 days exposure to 0.5 M NaCl (Fig. 26). This result may be explained by a mechanism in which the modified surface layer act as barrier to the movement of ions, retarding the cathodic reactions of oxygen reduction on the surface/solution interface. Due to the lack of a cathodic driving force, the dissolution of Al in the scratch is therefore reduced.

4.2.2 Properties of Modified Surface Layers

Cathodic and anodic polarization curves (Fig. 12 and 14) suggest that the modified surfaces do not allow either oxidation or reduction processes to occur at appreciable rates and show behavior which is typical of insulators. For surface modified Al 6061 in 0.5 M NaCl, i_p was less than 10^{-3} $\mu A/cm^2$. The cathodic polarization curve showed that at the same potential (-850 mV vs SCE), the cathodic current density was reduced to 0.08 $\mu A/cm^2$ for the modified sample, which was 20 times lower than that for the untreated sample (1.6 $\mu A/cm^2$) (Fig. 14). Apparently, the modified surface layers dose not provide easy paths for electrons and ions, and consequently the rates of oxygen reduction and anodic dissolution of Al are remarkably inhibited.

4.2.3 Effects of Ce and Mo in Modified Surface Layers

The impedance spectra for Al 6061 (Fig. 9), pure Al (Fig. 22) and Al 6013 (curves 3, 4 and 5 in Fig. 27) illustrate that modified surfaces with exceptional pitting resistance to localized corrosion can be produced by the Ce-Mo process. Since the surface modification process involved chemical treatments in Ce salt solutions and electrochemical treatment in a molybdate solution, Ce and Mo are expected to be incorporated into the surface layers. The EDS results suggest that Ce and Mo are present in the modified surface layers in fairly large amounts (Fig. 20). The concentration profiles obtained by AES showed that the concentration of Ce in the surface layers was as high as 25%, while the concentration of Mo was about 4 atomic % (Fig. 21). The presence of Mo species in the surface film serves to restrict the ingress of Cl^- and is considered to promote repassivation once pits have initiated. Their beneficial effects can not obtained with other analogous species such as borate as shown in Fig. 15 and 16. Experimental results have demonstrated that neither replacement of Na_2MoO_4 by borate buffer (pH = 7.4) nor replacement of hot Ce salt solutions by hot distilled water provide equal corrosion resistance for Al alloys similar to that produced by the Ce-Mo process.

Pit resistant surfaces produced by the Ce-Mo process are considered to be results of synergistic effects of Ce and Mo, rather than due to effects of Ce or Mo alone. It can be assumed that incorporated negatively charged Mo species retard the adsorption of Cl^- anions and prevent them from passing through the surface layers. The coexistence of Ce and Mo in the modified surface layers increases E_{pit} and also reduces the rate of oxygen reduction. A similar mechanism has been suggested to explain the role of Cr and Mo in pitting resistance of stainless steels [72,73].

4.3 Surface Modification of High-Cu Al Alloys

As mentioned earlier, when applying the Ce-Mo process to high-Cu Al alloys less satisfactory results were obtained. Cu-containing intermetallic compounds contained in the surface

layers apparently weaken the corrosion resistance of modified surfaces and/or interfere with the surface modification process. The presence of Cu-containing intermetallic compounds in the surface layers was shown to be the cause of failure of Al 7075-T73 treated with a chromate conversion coating in the salt spray test [74]. It becomes apparent that removing Cu from the outer surface layers of high-Cu Al alloys is necessary before application of corrosion protection methods. Corrosion protection of high-Cu Al alloys has been achieved by introducing Cu removal as a pretreatment step, which removes Cu from the outer surface layers without affecting the mechanical properties of the alloys.

Al alloys such as Al 2024 and Al 7075 usually contain significant amounts of constituent particles. It has been reported that localized corrosion takes place preferentially at Al_7Cu_2Fe on Al 7075 [71]. For Al 2024, the surface was found to contain numerous constituent particles such as Al-Cu-Fe-Mn and Al-Fe-Mg at a density of more than 300,000 per cm^2 with typical sizes between 5 and 20 μm. These particles act as cathodes and promote the dissolution of Al in their periphery, inducing pitting.

The effects of Cu-containing intermetallic compounds on pitting resistance were observed for modified Al 7075 exposed to 0.5 M NaCl. The surface modification process for as-received surfaces consisted of chemical treatment in Ce salt solutions combined with electrochemical treatment in a molybdate solution (Table VI). Upon exposure of the modified sample to 0.5 M NaCl, some corrosion spots due to localized dissolution of the surface film were observed after 4 days. Visually, these spots with dimensions of 60 μm displayed yellow-colored appearance. Elemental mapping indicated that Cu as an intermetallic compounds was located in the central areas of these spots with Ce oxides concentrated in their vicinities as shown in Fig. 31. The observed pattern can be explained by assuming that during the immersion the Ce salt solution, Cu as an intermetallic compounds acted as cathodes creating highly alkaline conditions in their peripheries where cathodic reduction of oxygen proceeds and Ce oxides/hydroxides precipitated. Since the effectiveness of the cathodes does not extend far away, Ce oxides are distributed in a ring pattern. According to Fig. 3.36, the typical size of Cu-containing intermetallic compounds is less than 10 μm, while the observed circular area is about 60 μm in diameter. Mo compounds were not uniformly distributed over the surface, but concentrated in the center of the ring where Cu-containing intermetallic compounds are located. This result might be due to increased current flow at sites containing Cu species during anodic polarization.

Significant improvements of the pitting resistance for Al 2024 and Al 7075 were achieved after introducing the Cu removal step prior to the Ce-Mo processes described in Tables VI and VII. During the electrochemical Cu removal step, Al 2024 was polarized at -55 mV vs. SCE in the Cu removal solution, while for Al 7075 a potential of -248 mV was applied. At these potentials, pure Cu was found to dissolve at high rates, while pure Al was passive as determined from their anodic polarization curves [75].

For modified Al 7075, no measurable corrosion was indicated by EIS for 30 day exposure to 0.5 M NaCl and at the end of the test, the corrosion spots observed for as-received Al 7075/Ce-Mo process were not detected by microscopic observation. The uniform corrosion rate was estimated to be about 0.07 μm/year. Apparently, applying the Cu removal process resulted in a surface close in chemical composition to that of low-Cu Al alloys. The elimination of localized corrosion was partially due to the lack of a potential driving force for pitting, i. e. reduction of the rate of the cathodic reaction [34].

In addition to the Cu removal step, the processing procedures were further optimized by exchanging step 2 and 3 in the original Ce-Mo process. The optimized process (Table VI) provides exceptional corrosion protection for Al 7075 as seen from Fig. 36. The improvement of the pitting resistance for the modified surfaces is considered to be partly due to minimized effect of Cl^- when the treatment in $CeCl_3$ was performed as the final step in the surface modification process. Since $CeCl_3$ solution contains Cl^- at three times greater concentration than Ce^{3+}, Cl^- can become entrapped in the surface layers during the formation of mixed Al-Ce oxides/hydroxides.

These entrapped Cl^- can initiate pits during subsequent exposure to NaCl. Performing anodic polarization in Na_2MoO_4 prior to treatment in $CeCl_3$ can reduce such effects, since Mo species reside preferentially at location where Cu-containing compounds are found as illustrated in Fig. 33.

Therefore, during treatment in $CeCl_3$ solution the adsorption of Cl^- can be inhibited and its penetration which would cause pitting can be prevented.

5. CONCLUSIONS

1. Localized corrosion in the form of pitting is one of the most common forms of failure of Al alloys in corrosive environments containing halides. For most Al alloys exposed to 0.5 M NaCl, E_{pit} and E_{corr} coincide and pitting occurs in less than one day. Cu-bearing Al alloys such as Al 2024 tend to be pitted more severely than Al alloys such as Al 6061 and Al 6013. Pitting initiates preferentially at constituent particles contained in the surface oxides due to galvanic coupling and at surface defects caused by mechanical damage and atmospheric corrosion.

2. EIS has been found to be a powerful tool for investigating localized corrosion and pit propagation processes on Al alloys. Pitting corrosion occurring on Al alloys can be detected by characteristic features of the EIS data. Once pits initiate, the impedance spectra change to a transmission line type of impedance at lower frequencies, and a second time constant in the phase angle plot became apparent in the corresponding frequency region. The pit propagation process is characterized by a decreasing impedance at intermediate frequencies and increasing phase angle corresponding to the second time constant at lower frequencies.

3. For Al alloys exposed to 0.5 M NaCl, the relationship $1/R^o_{pit} = a/t$ was obtained for pits growing at the open-circuit potential. Based on the assumption of hemispherical pits, the pit growth rate, expressed by the time dependence of the pit radius r, was found to follow the law $r = a' \log (t_p/t_o)$, suggesting that pit depth increases logarithmically with increasing pitting time t_p.

4. Three Ce-Mo processes have been developed as alternative approaches for chromate conversion coatings. These processes combine chemical treatments in Ce salt solutions with anodic polarization in a molybdate solution. The optimized modification procedure depends on alloy composition. For low-Cu Al alloys, corrosion resistant surfaces can be prepared by the Ce-Mo process described in Table V, while for high-Cu Al alloys the modified Ce-Mo processes (Table VI and VII) need be used to achieve optimized corrosion resistance.

5. The modified surface layer on Al 6061 contains both Ce and Mo and has excellent resistance to localized corrosion. Neither uniform corrosion nor pitting were indicated by EIS data and visual inspection. The very low passive current density and oxygen reduction rate suggest that movement of both cations and anions is reduced in the modified surface layers.

6. Ce and Mo can be incorporated into the surface oxide layers by the Ce-Mo processes. Ce

oxide/hydroxides are formed through chemical reactions during treatments in Ce salt solutions, while the incorporation of Mo species into the surface layers is obtained by a electrochemical reaction and chemical reaction between molybdate and aluminum oxide. The results of elemental mapping revealed that Ce precipitates and Mo species were enriched around constituent impurities.

Ce and Mo in the surface oxide layers act as barriers to the attack by aggressive ions such as Cl^- at these active sites, where without precipitation of Ce and Mo pits are likely to initiate.

7.　It has been shown that both Ce and Mo are needed for successful surface modification in order to make synergistic effects of Ce and Mo possible. Immersion in boiling water followed by polarization in a molybdate solution did not improve corrosion resistance. Replacement of the molybdate solution with borate buffer solution increased pitting resistance marginally. In addition, lowering of the molybdate concentration or reducing the polarization time decreased the corrosion resistance.

8.　For high-Cu Al alloys, Cu-containing intermetallic compounds in the surface layers reduce the resistance of modified surfaces to localized corrosion by inducing pitting in their peripheries due to galvanic coupling. An effective method for minimizing their detrimental effect can be the application of the Cu removal process as pretreatment step, which modifies the chemical composition of surface oxide layers closer to that for low-Cu Al alloys without affecting the mechanical properties of the alloys.

9.　By applying the Cu removal pretreatment step, corrosion resistant surfaces were obtained for Al 7075 in the modified Ce-Mo process. For surface modified Al 7075 no measurable corrosion was observed during exposure of 30 days to 0.5 M NaCl. Increased E_{pit} at constant E_{corr} indicates that the resulting surfaces are very resistance to pitting in aggressive environments. Surface analysis for the modified as-received Al 7075 has shown that Mo and Ce were concentrated at sites where Cu constituent particles are located, thereby reducing the extent and activity of local cathodes.

10.　For Al 2024, significant improvements in the resistance to localized corrosion were obtained when the Cu removal pretreatment was applied. Use of Ce acetate and elimination of $CeCl_3$ resulted in enhanced passivity of the modified surfaces in NaCl. Coexistence of Ce and Mo in the outer surface layers reduced susceptibility to localized corrosion by shifting E_{pit} in the noble direction at constant E_{corr}. The exceptional resistance to localized corrosion of modified surfaces on Al 2024 was related to synergistic effects of Ce and Mo indicated by capacitive impedance and increased E_{pit}.

ACKNOWLEDGMENT

6. REFERENCES

1. "Aluminum: Properties and Physical Metallurgy", edited by J. E. Hatch, American Society for Metals, Ohio, 1984, p. 321.
2. F. J. Boerio and D. J. Ondrus, J. Colloid Interface Sci., 139, 446 (1990).
3. G. E. Thompson and G. C. Wood, Treatise on Materials Science and Technology, 23, 205 (1983).
4. J. R. Galvele, Treatise on Materials Science and Technology, 23, 1 (1983).
5. W. Funke, in "Corrosion Protection by Organic Coatings", edited by M. W. Kendig, The Electrochemical Society, Proceedings Vol. 87-2, 1 (1987).
6. D. Thomas, Metal Finishing, 88(1), 417 (1990).
7. K. A. Korinek, in "Metals Handbook", 9th edition, Vol. 13, 389 (1982).
8. J. A. Treverton and N. C. Davies, Metals Technology, 4, 480 (1977).
9. U.S. Patent 2,796,370.
10. M. W. Kendig, A. J. Davenport and H. S. Isaacs, Corrosion Science, 34, 41 (1993).
11. H. A. Katzman, G. M. Malouf and G. W. Stupian, Applications of Surface Science, 2, 416 (1979).
12. K. Asami, M. Oki, G. E. Thompson, G. C. Wood and V. Ashworth, Electrochim. Acta, 32, 337 (1987).
13. H. J. Ashmead, J. Appl. Nutrition, 24, 8 (1972).
14. M. S. Vukasovich and J. P. G. Farr, Materials Performance, 25(5), 9 (1986).
15. N. Zaki, Metal Finishing, 88(6), 99 (1990).
16. J. Jefferies and B. Bucher, Materials Performance, 31(5), 50 (1992).
17. M. S. Vukasovich, Materials Performance, 29(5), 48 (1990).
18. B. R. W. Hinton, Metal Finishing, 89(9), 55 (1991).
19. C. M. Rangel and M. A. Travassos, Corrosion Science, 33, 327 (1992).
20. R. G. Buchheit, M. D. Bode and G. E. Stoner, Corrosion, 50, 205 (1994).
21. M. Sakashita and N. Sato, Corrosion, 35, 351 (1979).
22. W. C. Moshier and G. D. Davis, Corrosion, 46, 43 (1990).
23. R. R. Wiggle, V. Hospadaruk and E. A. Styloglou, Materials Performance, 20(6), 13 (1981).
24. M. A. Strainick, Corrosion/85, paper No. 380, NACE, 1985.
25. W. C. Moshier, G. D. Davis, J. S. Ahearn and H. F. Hough, J. Electrochem. Soc., 133, 1063 (1986).
26. R. C. Newman, Corrosion Science, 25, 331 (1985).
27. K. Sugimoto and Y. Sawada, Corrosion Science, 17, 425 (1977).
28. K. Kurosawa and T. Fukushima, Corr. Sci., 29, 1103 (1989).
29. B. A. Shaw, G. D. Davis, T. L. Fritz and K. A. Olver, J. Electrochem. Soc., 137, 359 (1990).
30. D. R. Gabe and S. E. Gould, Surface and Coatings Technology, 35, 79 (1988).
31. G. R. Bapu, J. Ayyapparaju, G. Devaraj and S. John, Metal Finishing, 89(3), 4 (1991).
32. A. H. Al-Saffer, V. Ashwarth, A. K. O. Bairamov, D. J. Chivers, W. A. Grant and R. P. M. Procter, Corrosion Science, 20, 1 (1980).
33. H. Kaesche, "Metallic Corrosion", NACE, 1985.
34. Y. Wang, "Corrosion Protection of Aluminum Alloys by Surface Modification Using Chromate-free Approaches", Ph. D. thesis, University of Southern California, November 1994.
35. H. Shih and F. Mansfeld, Corrsion, 45, 610 (1989).
36. F. Mansfeld, C. H. Tsai and H. Shih, ASTM, STP 1154, 186 (1992).
37. F. Mansfeld and H. Xiao, in Proc. "Biofouling and Biocorrosion in Natural Waters", ACS, Aug. 1992, Lewis Publ., 1994, p. 265.

38. F. Mansfeld and H. Xiao, J. Electrochem. Soc., 140, 2205 (1993).
39. F. Mansfeld and H. Xiao, Proc. 12th Int. Corrosion Cong., Houston, TX, 1993, p. 1388, NACE.
40. F. Mansfeld, Electrochim. Acta, 38, 1891 (1993).
41. F. Mansfeld and H. Shih, J. Electrochem. Soc., 135, 1171 (1988).
42. F. Mansfeld, S. Lin. S. Kim and H. Shih, J. Electrochem. Soc., 137, 78 (1990).
43. F. Mansfeld, Y. Wang and H. Shih, Electrochim. Acta, 37, 2277 (1992).
44. D. R. Arnott, N. E. Ryan, B. R. W. Hinton, B. A. Sexton and A. E. Hughes, Appl. Surf. Sci., 22/23, 236 (1985).
45. D. R. Arnott, B. R. W. Hinton and N. E. Ryan, Corrosion, 45, 12 (1989).
46. A. J. Aldykiewicz, Jr. H. S. Isaacs and A. J. Davenport, Ext. Abstr. 185th Scociety Meeting, The Electrochemical Society, San Francisco, CA, 1994, paper No. 43.
47. G. H. Cartledge, Corrosion, 24, 223 (1968).
48. Y. Okamoto and T. Imanaka, J. Phys. Chem., 92, 7102 (1988).
49. G. H. Bailey, Engineering, 95, 374 (1912).
50. J. O'M. Bockris and Lj. V. Minevski, J. Electroanal. Chem., 349, 375 (1993).
51. R. T. Foley, Corrosion, 42, 277 (1986).
52. B. N. Stirrup, N. A. Hampson and I. S. Midghley, J. Appl. Electrochem., 5, 229 (1975).
53. Z. S. Smialowska, Corrosion, 27, 223 (1971).
54. J. Zahavi and M. Metzger, in "Localized Corrosion", edited by R. W. Staehle, B. F. Brown, J. Kruger and A. Agrawal, International Corrosion Conference Series, Houston, TX, 1974, p. 547, NACE.
55. K. Nisancioglu and H. Holtan, Corr. Sci., 18, 835 (1978).
56. A. Broli and H. Holtan, Corr. Sci., 13, 237 (1973).
57. N. Nilson and E. Bardal, Corr. Sci., 17, 635 (1977).
58. J. Augustynski, in "Passivity in Metals", edited by R. P. Frankenthal and J. Kruger, The Electrochem. Soc., Princeton, NJ, 1978, p. 989.
59. F. Mansfeld, S. Lin, S. Kim and H. Shih, Corrosion, 45, 615 (1989).
60. F. Mansfeld, Electrochim. Acta, 35, 1533 (1990).
61. F. Hunkeler and Böhni, Werkst. Korros., 32, 129 (1981).
62. F. Hunkeler and Böhni, Corrosion, 37, 645 (1981).
63. F. Hunkeler and Böhni, Werkst. Korros., 34, 68 (1983).
64. F. Hunkeler and Böhni, Corrosion, 40, 534 (1984).
65. B. R. W. Hinton, D. R. Arnott and N. E. Ryan, Metals Forum, 7(4), 211 (1984).
66. D. R. Arnott, B. R. W. Hinton and N. E. Ryan, Corrosion/86, paper No. 197, NACE, 1986.
67. B. R. W. Hinton, N. E. Ryan, D. R. Arnott, P. N. Trathen, L. Wilson and B. E. Williams, Corrosion Australasia, 10(3), 12 (1985).
68. B. R. W. Hinton, Corrosion/89, paper No. 170, NACE, 1989.
69. D. R. Arnott, B. R. W. Hinton and N. E. Ryan, Corrosion, 45, 12 (1989).
70. F. Mansfeld and Y. Wang, unpublished results.
71. G. D. Davis, T. L. Fritz, B. J. Rees, B. A. Shaw and W. C. Moshier, "A Study of the Influence of Alloying Additions of the Passivity of Aluminum", Annual report to Office of Naval Research, Contract No. N00014-85-C-0638, March, 1991.
72. G. Okamoto and T. Shibata, "Passivity and the Breakdown of Passivity of Stainless Steel", in "Passivity of Metals", edited by R. P. Frankenthal and J. Kruger, The Electrochemical Society Inc., Princeton, New Jersey, 1978, p. 646.
73. M. Kendig and C. Thomas, J. Electrochem. Soc., 139, 1103 (1992).
74. F. Mansfeld, "Optimization of Chromate Conversion Coatings on Al 7075-T73", Final Report to Sandia National Laboratories, Contract No. 57-2928, December, 1989.
75. F. Mansfeld, L. Kwiatkowski and S. Lin, unpublished results.